Chapter 3
Southern Victoria Land; Basement Rocks

The geological architecture of the Transantarctic Mountains in Table 3.1 is deceptively simple because it consists of only four suites of rocks which are separated by unconformities and intrusive contacts. The most pervasive and longest erosional interval is represented by the Kukri Unconformity, also called the Kukri Peneplain. This erosional surface separates the rocks of the underlying basement complex from the overlying sedimentary rocks of the Beacon Supergroup of Early Devonian to Late Triassic age and the dolerite sills of the Ferrar Group that intruded the Beacon rocks during the Middle Jurassic. The Beacon rocks are locally overlain by the sheet-like flows of the Kirkpatrick Basalt which formed where Ferrar magmas were erupted through fissures. The most recent episode of volcanic activity started during the Miocene, less than about 25 million years ago, when alkali basalt lava and pyroclastics of the McMurdo Volcanic Group were erupted through vents at numerous sites in the Transantarctic Mountains from northern Victoria Land (Cape Adare) to Mt. Early located close to the South Pole (LeMasurier and Thomson 1990). Mt. Erebus on Ross Island is the last of these Tertiary volcanoes to remain active at the present time (Kyle 1995).

The basement complex which underlies the Transantarctic Mountains along their entire length is exposed in a broad region along the coast of Victoria Land and along the edge of the Ross Ice Shelf all the way to the Horlick Mountains and beyond (Grindley 1981; Laird and Bradshaw 1982). It consists of sedimentary and volcanic rocks that were intensely folded, regionally metamorphosed, and intruded by granitic rocks of the Granite Harbor Intrusives (Table 3.1). The metamorphism of the sedimentary and volcanic rocks that occurred during the Ross Orogeny was sufficiently severe to convert these rocks locally into paragneisses and to generate the granitic magmas that intruded the volcano-sedimentary complex between 530 and 470 million years ago (i.e., Early Cambrian to Middle Ordovician) based on the Geologic Time Scale of the International Union of Geological Sciences issued in 2002 (IUGS 2002).

The rocks of the basement complex formed and were subsequently altered while Antarctica was an integral part of the supercontinent Gondwana, which contained all of the southern continents we know today. The lithologic and structural diversity of the basement rocks is compounded by their fragmentary exposure along the Transantarctic Mountains. Therefore, we have chosen to describe the basement rocks in each of the five segments defined in Fig. 3.1 and we will also use these subdivisions of the Transantarctic Mountains to describe the rocks that overlie the basement complex.

Rocks of Precambrian age are also exposed along the coast of East Antarctica in Fig. 3.2 and under the ice sheet of East Antarctica. The rocks of the subglacial crust are known only in terms of their geophysical properties that have been measured during surface traverses as well as by airborne and satellite surveys. The Precambrian rocks of the subglacial crust and of the coastal areas of East Antarctica have not been correlated with the basement rocks of the Transantarctic Mountains except in terms of their ages as measured by radiogenic-isotope geochronometry (Faure and Mensing 2005).

The geology of all parts of Antarctica was compiled by Craddock (1969a) and a group of 24 collaborators in the form of color-coded geological maps and associated text. This important work contains 18 geological maps that include all major outcrop areas of Antarctica. The geology of the Transantarctic Mountains is presented in six of these maps (i.e., 5, 13, 14, 15 16, and 17). Although these maps were published more

G. Faure and T.M. Mensing, *The Transantarctic Mountains: Rocks, Ice, Meteorites and Water*,
DOI 10.1007/978-90-481-9390-5_3, © Springer Science+Business Media B.V. 2010

Table 3.1 Simplified geological architecture of the continental crust of the Transantarctic Mountains in southern Victoria Land

Rock types	Geologic unit	Geologic time, Ma[a]
Alkali-rich volcanic rocks	McMurdo Volcanic Group	Miocene to Holocene 25 to 0.0
Dolerite sills and basalt flows	Ferrar and Kirkpatrick groups	Middle Jurassic 176.8 ± 1.8[b]
Sandstone, shale, tillite, coal	Beacon Supergroup	Early Devonian to Late Triassic 417 to 205
~~	Kukri Unconformity	~~~~~~~~~~~~~~~~~~~~~~~~~~~~
Granitic plutons and late-stage dikes	Granite Harbor Intrusives	Late Cambrian to Middle Ordovician
Metamorphosed and folded volcano-sedimentary complexes	Ross Supergroup Koettlitz and Skelton groups	Precambrian to Late Cambrian

[a] Ma = millions of years ago (mega anna)

[b] Heimann et al. (1994)

than 35 years ago and although they are now available only in private collections and certain libraries, they remain a useful resource for geologists who are interested in the geology of Antarctica.

In addition, the proceedings volumes of SCAR Meetings and of International Gondwana Symposia listed in Appendices 1.10.4 and 1.10.5 contain a wealth of information about the geology of the continent, as do the volumes of the Antarctic Research Series of the American Geophysical Union (Appendix 1.10.6) and the publications of the Geological Society of America (Appendix 1.10.7). The accumulated information about the geology of Antarctica has been summarized and interpreted by Gunn (1963), Ford (1964), Fairbridge (1975), Rowley (1983), Swithinbank (1988), Tingey (1991, 1996), Gamble et al. (2002), and others.

The Transantarctic Mountains have been mapped by geologists from New Zealand, the United Kingdom, USA, Australia, Germany, the USSR, and Italy. Several of these nations have established research stations on Ross Island and in Victoria Land. The fieldwork during the IGY (1957/58) and in the decades that followed was done by use of dogsleds (Herbert 1962) and snowmobiles, as well as by man-hauling sleds (Nichols 1963; Wade et al. 1965), and even by backpacking (McKelvey and Webb 1962) until helicopters and fixed-wing aircraft became available for support of geological field parties. The results of studies by scientists from New Zealand were published in ten special issues of the New Zealand Journal of Geology and Geophysics (Collins 1962, 1963, 1965, 1967; Bodley 1968). All of the publications arising from work done under the aegis of the New Zealand Antarctic Research Programmes between 1956 and 1964 were listed by Quartermain (1963, 1965). The post-IGY review papers of the geology of the Transantarctic Mountains include the work of Harrington (1958), Gunn and Warren (1962), Gunn (1963), Grindley and Warren (1964), and Schmidt (1966).

The amount of information that has accumulated about the geology of the Transantarctic Mountains is very large. Even when only the basement rocks are considered, the information in published reports is overwhelming and is difficult to fit into a coherent tectonic model, partly because the stratigraphy, structural deformation, and metamorphic grade of the rocks vary regionally and because the tectonic environment of the area of deposition of the basement rocks is obscured by the present configuration of Antarctica. Nevertheless, several authors have proposed explanations for the tectonic evolution of Antarctica in the context of the assembly of Gondwana (e.g., Hamilton 1967; Elliot 1975; Laird 1981; Grikurov 1982; Findlay et al. 1984, 1993; Allibone et al. 1993a, b; Stump 1995; Encarnación and Grunow 1996; Fűtterer et al. 1996).

The most successful synthesis of the data pertaining specifically to the basement rocks of the Transantarctic Mountains was published in a book by Stump (1995) whose tectonic model is based on the insight that the basement rocks were deposited along a passive margin of Gondwana after the break-away of Laurentia from Rodinia during the Neoproterozoic (Bell and Jefferson 1987; Moores 1991).

According to this concept, the paleo-Pacific margin of Gondwana in Fig. 3.3 was activated when a subduction zone developed along it (Ferracioli et al. 2002). The resulting subduction of the oceanic crust caused compression of the sediment and volcanics that had accumulated during the passive-margin phase and resulted in magmatic activity that started around 600 Ma. The intrusion of syntectonic plutons into the Ross

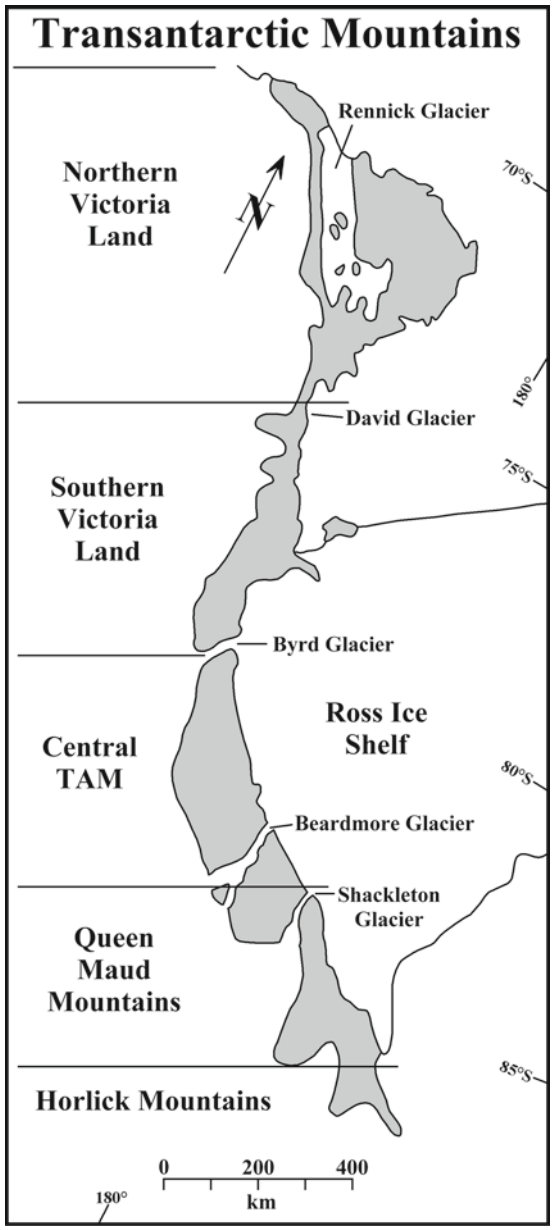

Fig. 3.1 For the purposes of this presentation the Transantarctic Mountains have been subdivided into five segments which are defined in this diagram. The shaded outcrop areas expose the basement rocks that are the subject of the following series of chapters. North in this and other maps in this book is at the top (Adapted from Stump et al. 2006)

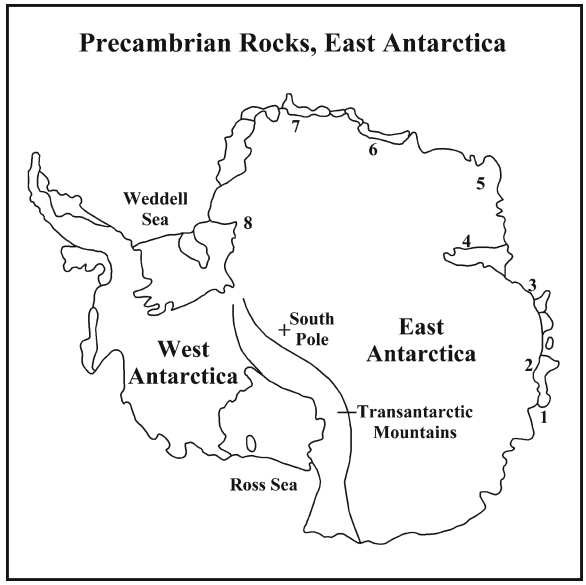

Fig. 3.2 Precambrian basement rocks are exposed along the coast of East Antarctica and in the mountain ranges along the edge of the ice sheet. The localities that are identified by number include: 1.Vincennes Bay, 2. Bunger Hills (Queen Mary Coast), 3. Vestfold and Larsemann Hills 4. Prince Charles Mountains (MacRobertson Land) 5. Enderby Land; 6. Sor Rondane Mountains 7. New Schwabenland (Queen Maud Land), and 8. Shackleton Range. Precambrian rocks also form the crust of East Antarctica that is covered by the ice sheet (Adapted from Stonehouse 2002; Craddock 1982)

Mountains ended at about 500 Ma and was followed by post-tectonic magmatic activity until about 460 Ma. Grunow et al. (1996) suggested that the magmatic activity along the Transantarctic Mountains coincided with and may be related to the Pan-African deformation event that occurred in Africa, southern India, Sri Lanka, and those parts of South America that were joined to Africa prior to the opening of the Atlantic Ocean.

The model of the origin and tectonic evolution of the Ross orogen described by Stump (1995), Grunow et al. (1996), Encarnación and Grunow (1996), Borg and DePaolo (1991, 1994), and Dalziel (1991) places the Transantarctic Mountains into the context of the assembly and subsequent dispersal of Gondwana which began when Laurentia split from Rodinia. Many details about the subsequent evolution of the resulting rift margin of Gondwana are still open for discussion, including the accretion of "suspect" terranes (Bradshaw et al. 1985) and the deposition of marine carbonate rocks along a coast that was presumably experiencing compression and magmatic activity resulting from subduction of oceanic crust under the continental margin of Gondwana (Stump 1995). These and other topics related to the formation of the Transantarctic Mountains will be discussed in subsequent chapters of this book.

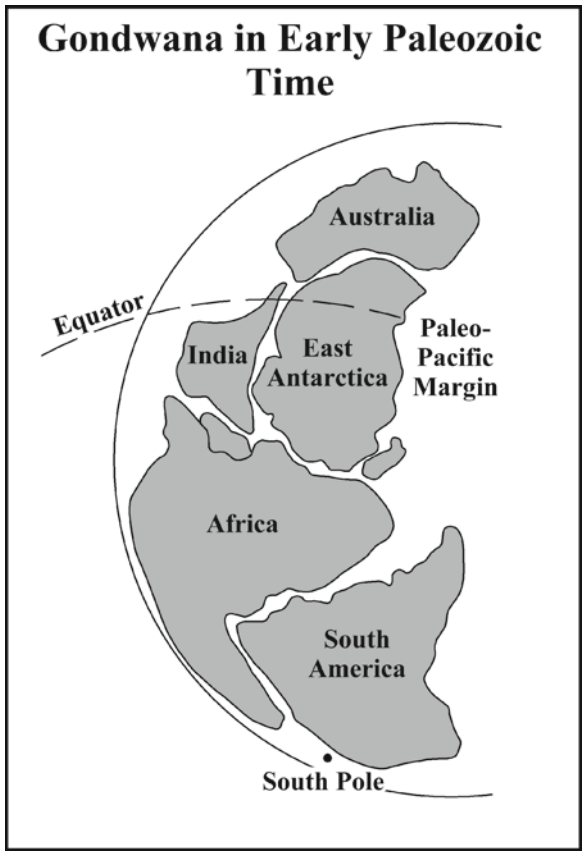

Fig. 3.3 The rifting of the supercontinent Rodinia during the Neoproterozoic Era split the future East Antarctic craton and caused Laurentia (the continental fragment that split from East Antarctica) to drift away. The newly formed paleo-Pacific coast of Gondwana, including East Antarctica, thereby became a passive margin along which detrital sediment was deposited by turbidity currents. Subsequently, the turbidites were folded and metamorphosed when an active subduction zone developed along the coast of Gondwana in early Paleozoic time. The deformation of the sedimentary rocks and the formation of granitic magma formed the Ross orogen which later became the basement upon which the sedimentary rocks of the Beacon Supergroup were deposited (Adapted from Encarnación and Grunow 1996)

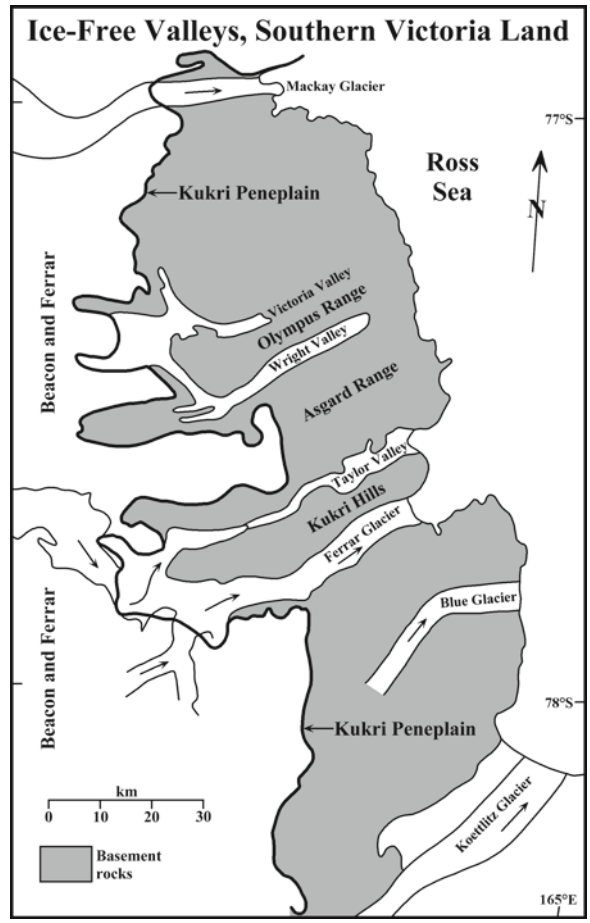

Fig. 3.4 Outcrop belt of the basement rocks along the coast of southern Victoria Land in the area of the ice-free valleys and adjacent to the Koettlitz Glacier. The trace of the Kukri Peneplain divides the area where basement rocks are exposed to the east from the area to the west where the basement rocks are overlain by the sandstones of the Beacon Supergroup (Devonian to Triassic) and by the sills of the Ferrar Dolerite (Middle Jurassic). The basement rocks in this part of the Transantarctic Mountains consist of the quartzo-feldspathic metasediments (Neoproterozoic) and marine carbonates (Cambrian) of the Ross Supergroup which was intruded by the Granite Harbor Intrusives consisting of syntectonic and post-tectonic granitic rocks ranging in composition from granite to granodiorite and diorite (Adapted from the geologic map of Craddock (1969 a) and Warren (1969))

The basement rocks of *southern Victoria Land* defined in Fig. 3.1 are exposed in an irregular belt along the coast and consist primarily of the Granite Harbor Intrusives of Cambrian age which intruded the folded metasedimentary rocks of the Ross Supergroup of Cambrian and Neoproterozoic age (Warren 1969). This outcrop belt extends from the David Glacier south to the Byrd Glacier and includes the basement rocks that are exposed in the ice-free Victoria, Wright, and Taylor valleys in Fig. 3.4. Another large exposure of basement rocks included in Fig. 3.4 occurs between the Ferrar and the Koettlitz glaciers. A third area of exposure of Granite Harbor Intrusives in the Brown Hills between the Carlyon and Darwin glaciers and in the Britannia Range, located between the Koettlitz and Byrd glaciers (Grindley and Laird 1969) is not shown in Fig. 3.4.

3.1 Ice-Free Valleys

The ice-free valleys of southern Victoria Land in Fig. 3.4 were the first part of the Transantarctic Mountains to be studied by geologists during Scott's Discovery Expedition (1901–1904) which included the geologist Hartley T. Ferrar and the surveyor and navigator Albert B. Armitage. A few years later, Shackleton's Nimrod Expedition (1907–1909) included the geologists T. William E. David, Douglas Mawson, Raymond E. Priestley, and Sir Philip L. Brocklehurst. After returning from the Nimrod Expedition with Shackleton, Raymond Priestley joined Scott's Terra Nova Expedition (1910–1913) along with Frank Debenham, Charles S. Wright, and T. Griffith Taylor.

3.1.1 Topography

The ice-free valleys in Fig. 3.4 consist of several parallel ice-carved valleys that are separated from each other by mountain ranges. The central area of this region is occupied by the Wright and Taylor valleys which are separated from each other by the Asgard Range. North of Wright Valley is a large ice-free area which includes the Victoria, Barwick, Balham, and McKelvey valleys which are separated from the Wright Valley by the Olympus Range. The valley of the Ferrar Glacier, located south of Taylor Valley, is separated from it by the Kukri Hills.

Wright Valley in Fig. 3.5 is ice-free because only a small amount of ice from the polar plateau is presently entering it via the Airdevronsix Icefall which feeds the Wright Upper Glacier. Even smaller amounts of ice are flowing into Barwick Valley by way of the Webb Glacier and into Victoria Valley via the Victoria Upper Glacier in Fig. 3.6. The starvation of the outlet glaciers that once occupied Wright Valley and the Victoria Valleys in the past was caused by a decrease of the thickness of the East Antarctic ice sheet combined with the presence of subglacial bedrock obstructions along the ice-covered western slope of the Transantarctic Mountains in this area (Calkin 1974; Studinger et al. 2004). In addition, Bull (1966) demonstrated that the ice-free areas of southern Victoria Land absorb more solar heat than neighboring areas which are still ice covered. He concluded that the increased heat-absorption, combined with the small amount of annual precipitation, is currently preventing snow from accumulating in the ice-free valleys of southern Victoria Land. However, the "U-shaped" profiles of these valleys and the presence of glacial deposits within them leaves no doubt that they were occupied by glaciers in the past (Péwé 1960; Denton et al. 1970; Mayewski and Goldthwait 1985). The aridity of the climate in the ice-free (or "dry") valleys was previously demonstrated by the legendary Robert Nichols, Professor of Geology, at Tufts University of Massachusetts who introduced many of his students to the glacial geology and geomorphology of southern Victoria Land (Nichols 1963). Taylor Valley in Fig. 3.7 actually does contain a glacier that still flows from the polar plateau and terminates within that valley, most of which is ice-free, whereas the Ferrar Glacier continues to transport ice from the polar plateau to New Harbor on McMurdo Sound.

The rugged topography of the Transantarctic Mountains of southern Victoria Land originated by erosion of the landscape by glaciers that have sculpted the mountains into horns separated by cirque basins. For example, the summit plateau of the Olympus Range in Fig. 3.5 contains a large number of glacial horns including: Mt. Theseus (1,829 m), Mt. Peleus (1,790 m), Mt. Jason, Mt. Hercules, Mt. Aeolus, Mt. Boreas (2,180 m), Mt. Dido (2,070 m), Mt. Circe, and Mt. Electra. All of these peaks as well as the mountain range itself (i.e., Olympus) were named after characters in Greek mythology (Houtzager 2003). The glacial horns of the Asgard Range recall the names of deities in Norse mythology who had residences in Asgard: Odin, Thor, Baldr, the Valkyries, and Loki (spelled "Loke" on the USGS map ST 57–60/6*). The highest peaks of the ice-free valleys occur along the edge of the polar plateau, including Mt. Feather (2,985 m), Shapeless Mountain (2,739 m), Tabular Mountain (2,700 m), and Mt. Bastion (2,530 m).

Certain places in the ice-free valleys have been designated Sites of Special Scientific Interest (SSSIs), in order to protect ongoing scientific research or to preserve them in pristine condition for possible future study. This action was taken by the seventh Antarctic Treaty Consultative Meeting (ATCM VII) in 1972 and is contained in Recommendation VII-3 (Stonehouse 2002, p. 369). The SSSI sites in the ice-free valleys are: Barwick Valley (Fig. 3.6), the area between the Canada Glacier and Lake Fryxell (Taylor Valley), and the Linnaeus Terrace

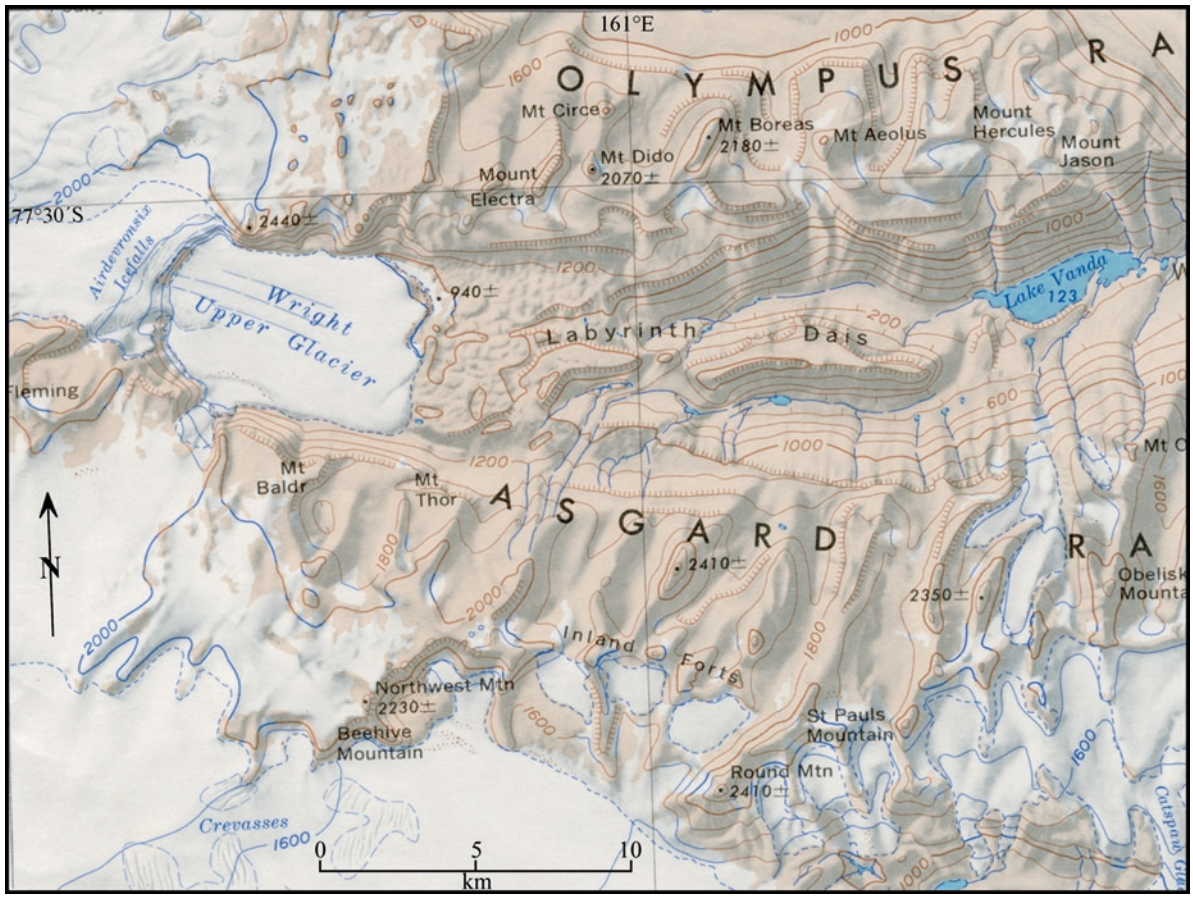

Fig. 3.5 The western end of Wright Valley in southern Victoria Land is framed by the Olympus Range in the north and the Asgard Range in the south. Ice from the East Antarctic ice sheet of the polar plateau enters the valley via the Airdevronsix icefall and forms the Wright Upper Glacier. The Labyrinth at its base was carved by meltwater streams flowing under pressure at the base of a glacier that once filled the Wright Valley. Lake Vanda is perennially covered by ice except for a moat of open water that forms during the summer months in December and January. In contrast to its icy surface, Lake Vanda contains a layer of hot brine at the bottom that is heated by sunlight which penetrates the ice and overlying clear water (Excerpt from the Taylor Glacier, Antarctica topographic map (ST 57–69/5; 77198-S1-TR-250; revised 1988) published by the U.S. Geological Survey, Denvery, Colorado)

(77°36'S, 161°05'E,). The Linnaeus Terrace was protected because of the presence of endolithic algae and lichens in the Beacon Sandstone at that site (Friedmann et al. 1988).

3.1.2 Geology

The basement rocks of the ice-free valleys of southern Victoria Land, including the area between the Ferrar and the Koettlitz glaciers farther south in Fig. 3.4, exemplify the structural complexity, lithologic diversity, regional metamorphism, and magmatic activity of the Ross orogen. Therefore, the geology of this area is presented in sufficient detail to serve as the type example for the basement rocks exposed elsewhere along the Transantarctic Mountains.

The geology of the Victoria and Wright valleys in Fig. 3.8 was mapped by P.N. Webb and B.C. McKelvey during the austral summers of 1957 and 1958, respectively (Webb and McKelvey 1959; McKelvey and Webb 1962). Their work, together with that of Harrington (1958), Gunn and Warren (1962), and Grindley and Warren (1964), set the stage for the ongoing study of the geology of the Transantarctic Mountains (e.g., Findlay et al. 1984; Allibone et al. 1993a, b; Encarnación and Grunow 1996).

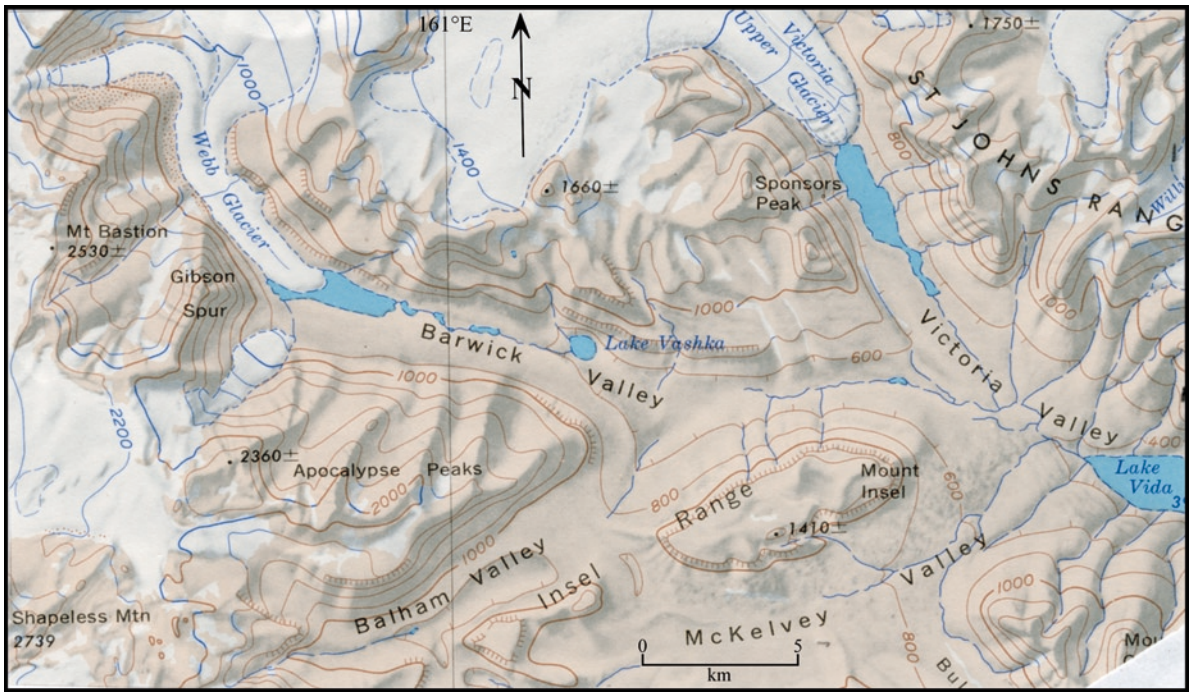

Fig. 3.6 The Balham, Barwick, Victoria, and McKelvey valleys of southern Victoria Land are ice-free because the flow of ice from the polar plateau via the Webb Glacier and the Upper Victoria Glacier is currently restricted. These valleys therefore expose metamorphic and granitic igneous rocks of the basement complex overlain unconformably by the Lower Devonian sandstones of the Beacon Supergroup. The Vida Granite in this area is named after Lake Vida in Victoria Valley. Meltwater lakes occur at the foot of the Webb and Upper Victoria Glaciers. The Barwick Valley also contains Lake Vashka (Excerpt from the Taylor Glacier, Antarctica topographic map (ST 57–69/5; 77198-S1-TR-250; revised 1988) published by the U.S. Geological Survey, Denver, Colorado)

McKelvey and Webb (1962) reported that large parts of *Wright Valley* are underlain by tightly folded metasedimentary rocks of the Asgard Formation which they assigned to the Neoproterozoic-Early Cambrian Skelton Group of the Ross orogen. Although Findlay et al. (1984) later abolished the Asgard Formation, it remains a valid local stratigraphic unit. The metasedimentary rocks of the Asgard Formation were intruded by the syntectonic Wright Intrusives consisting of: Theseus Granodiorite, Loke Microgranite, Dais Granite, and Olympus Granite-Gneiss. After the main phase of compressive deformation (i.e., the Ross Orogeny), the Asgard Formation and the Wright Intrusives were invaded by the Vida Granite and dikes of Vanda Lamprophyre and Porphyry which together constitute the suite of Victoria Intrusives of McKelvey and Webb (1962). In a larger context, the Wright and Victoria intrusives are the local representatives of the Granite Harbor Intrusives of southern Victoria Land.

More recently, Allibone et al. (1993a, b) and Cox (1993) identified 15 major granitic plutons in southern Victoria Land and proposed a new set of names for them because the lithologic character of the plutons is sufficiently diverse to resemble several of the intrusives previously named by McKelvey and Webb (1962). The classification of Allibone et al. (1993a, b) consists of three groups of intrusives:

1. Elongate, *concordant* plutons, which range from monzodiorite to granodiorite, are relatively undeformed and contain aligned K-feldspar megacrysts, hornblende, biotite, and mafic inclusions. These plutons were emplaced between 589 and 490 million years ago at deep levels during the metamorphism to the upper amphibolite facies of the metasedimentary rocks of the Asgard Formation.

   The names of these concordant plutons are: Bonney, Denton, Cavendish, and Wheeler.

Fig. 3.7 Taylor Valley in southern Victoria Land still contains a glacier that discharges meltwater into Lake Bonney. Ice from the East Antarctic ice sheet enters both the Taylor and Ferrar valleys but only the Ferrar Glacier actually reaches McMurdo Sound. The Rhone Glacier descends from the valley wall on the right. A thick sill of the Ferrar Dolerite is exposed farther up the valley (Photo by Rebecca Witherow reproduced by permission)

2. Elongate, *discordant* plutons are composed of equigranular, homogeneous biotite granodiorite and granite, and were intruded at shallow depth in the crust at 490 million years ago.

   The names of these discordant plutons are: Hedley, Valhalla, St. Johns, and Suess.

3. Discordant ovoid plutons that cut and are themselves cut by the Vanda dikes of mafic and felsic porphyry. These plutons were emplaced at shallow depth between 486 and 477 million years ago and range in composition from monzonite to granite. Some of these plutons contain K-feldspar megacrysts that resemble the texture of the oldest concordant plutons.

   The names of these youngest discordant plutons are: Pearse, Nibelungen, Orestes, Brownworth, Swinford, and Harker.

The new terminology for the magmatic rocks of the ice-free valleys was adopted by Encarnación and Grunow (1996) and was evaluated by Stump (1995) in the light of the nomenclature used in the literature that preceded the publications of Allibone et al. (1993a, b). These authors tried to improve the mapping of the ice-free valleys of southern Victoria Land by examining the contacts of individual plutons and by applying geochemical criteria that were not available to the geologists who worked in the valleys during the IGY and in the decade that followed. The new geologic map of Allibone et al. (1993a, b) is based on interpolations

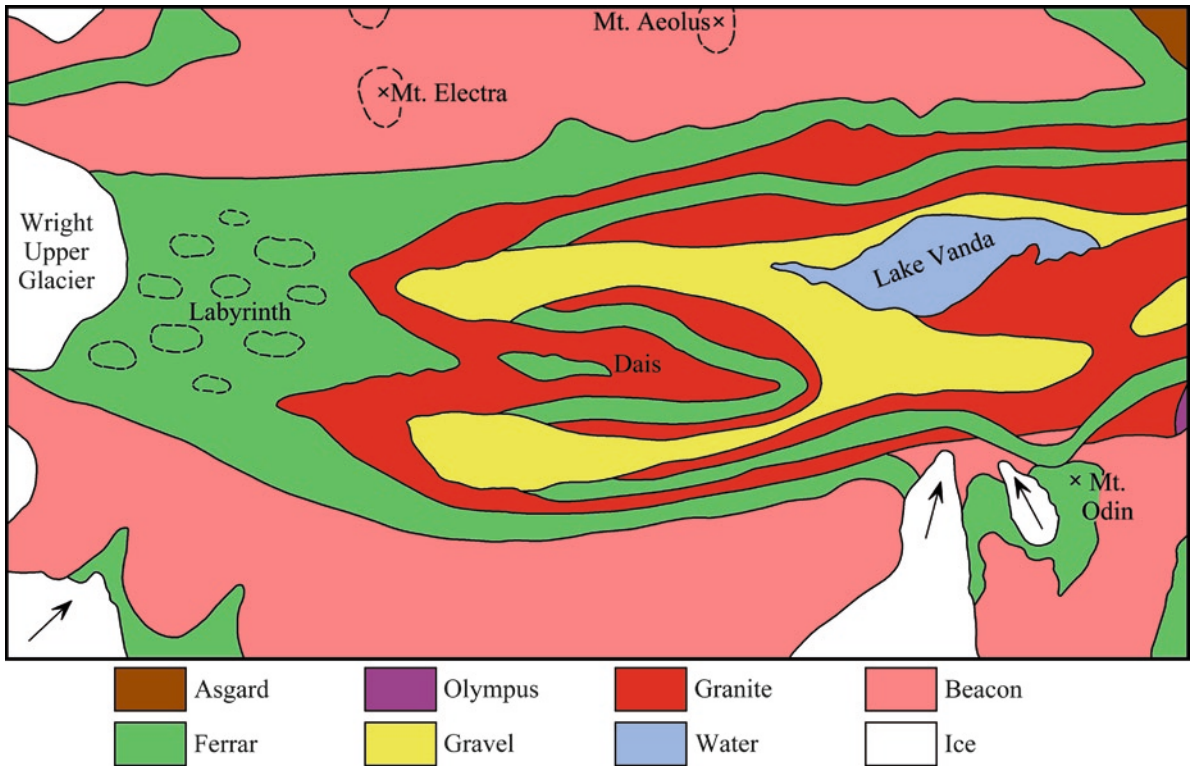

Fig. 3.8 Geologic map of the western Wright Valley in southern Victoria Land. This area is included in Fig. 3.5 (Adapted from McKelvey and Webb 1962)

between outcrops of plutonic basement rocks, which are extensively covered by the sandstones of the Beacon Supergroup and by the sills of the Ferrar dolerite. These interpolations between outcrops can be tested in the future by diamond drilling at selected sites in order to confirm the continuity of the underlying plutons beneath the cover rocks and glacial deposits.

The *Asgard Formation* of Wright Valley described by McKelvey and Webb (1962) consists of interbedded marbles, hornfels, and schists that grade locally into paragneiss and migmatite close to contacts with plutons of the Wright Intrusives. The type locality of this formation is the south wall of Wright Valley between Mt. Loke and Mt. Valkyrie.

The marbles are coarse-grained white rocks that disintegrate readily and therefore are rarely found in talus or moraines. They are composed of twinned grains of calcite with minor graphite and diopside. The metamorphic rocks classified as hornfels by McKelvey and Webb (1962) are composed of red garnet (13 mm) and fine-grained green diopside with minor amounts of quartz. Some specimens contain scapolite, diopside, and sphene in contact with the marble layers. The most common schist layers are composed of quartz and feldspar, but the schist locally contains plagioclase, biotite, and hornblende. The metasedimentary rocks of the Asgard Formation contain intercalated intrusive granitic orthogneisses (Allibone et al. 1993a) which form the Olympus Granite-Gneiss of McKelvey and Webb (1962). These orthogneisses are prominent along the north wall of Wright Valley east of Bull Pass. In this exposure, the foliation of the gneiss is aligned parallel with the strike of the Asgard Formation, inclusions of which occur in the transition zone within the gneiss. The relationship of the Olympus Granite-Gneiss to the other lithologies of the basement complex is uncertain although McKelvey and Webb (1962) considered the Olympus Granite-Gneiss to be one of the Wright Intrusives.

The development of augen gneiss by metasomatism of quartzo-feldspathic gneiss which formed by regional metamorphism during intense deformation of greywacke

and sandstone was described by Smithson et al. (1971a, b) as an explanation for the gradational relationship between the Olympus Granite-Gneiss and the interbedded metasedimentary rocks of the Asgard Formation. Smithson et al. (1971c) also proposed that amphibolite reaction rims can form by metasomatic introduction of iron and magnesium coupled with the loss of calcium from diopside granofels, which is a medium- to coarse-grained granoblastic metamorphic rock with little or no foliation or lineation (Jackson 1997). The conversion of metasedimentary rocks into crystalline gneiss complexes is a characteristic of the Ross orogen that forms the basement complex of the Transantarctic Mountains (Grindley 1971, 1981).

The other members of the Wright Intrusives described by McKelvey and Webb (1962) are distinguished primarily by their texture, mineral composition, and bulk chemistry. The relation of these units to the terminology of Allibone et al. (1993a, b) is indicated in Table 3.2. Until the new terminology of the plutonic rocks in the ice-free valleys has been tested in the field and is confirmed by drilling and/or additional mapping, we will continue to use the traditional nomenclature. However, we consider that the Asgard Formation of McKelvey and Webb (1962) is largely correlative with the amphibolite-grade metasediments north of the Skelton Glacier and we will therefore refer to it as the Asgard Formation (Koettlitz Group) or simply as Koettlitz Group metasediments.

Table 3.2 Relation of the terminology of Allibone et al. (1993a, b) to the classification of the igneous and metamorphic rocks in Victoria, Wright, and Taylor valleys by Allen and Gibson (1962), McKelvey and Webb (1962), and Haskell et al. (1965a), respectively

Allibone et al. (1993a, b)	Previous classification
Bonney pluton	Olympus Granite-Gneiss and Dais Granite (Wright Valley) Larsen Granodiorite (Taylor Valley)
Denton pluton	Olympus Granite-Gneiss (Wright Valley)
Wheeler pluton	Larsen Granodiorite (Taylor Valley) Dais Granite (Victoria Valley)
Catspaw pluton	Irizar Granite (Taylor Valley)
St. Johns pluton	Vida Granite (Victoria Valley)
Hedley pluton	Vida Granite (Ferrar Valley)
Suess pluton	Larsen Granodiorite
Valhalla pluton	Olympus Granite and Dais granite (Wright Valley)
Biotite granitoid dikes	Theseus Granodiorite (Wright and Taylor Valleys)

The *Dais Granite* is exposed in the so-called Dais west of Lake Vanda close to the western (inland) end of Wright Valley. It is coarsely foliated parallel to the strike of the Koettlitz-Group metasediments and of the Olympus Granite-Gneiss. The Dais Granite is characterized by being porphyritic with large phenocrysts of orthoclase in a coarse matrix of oligoclase, hornblende, biotite, and quartz. Allanite, zircon, iron oxide, and apatite are present as accessory minerals. The Dais Granite has the composition of an adamellite that grades locally into alkali granite (Appendix 3.7.1).

The *Loke* (or Loki) *Microdiorite* occurs as dikes up to 2.5 m wide that intrude the Olympus Granite-Gneiss at Mt. Loke (Loki) and east of Mt. Theseus. The microdiorite contains up to 25% biotite and 15% green hornblende, as well as plagioclase, orthoclase, and quartz (Appendix 3.6.1).

Dikes of *Theseus Granodiorite* intrude the metasedimentary rocks of the Koettlitz Group and all of the other members of the Wright Intrusives. The type locality of the Theseus Granodiorite is on the north wall of Wright Valley between Mt. Theseus and Bull Pass. Similar intrusives of grey biotite granite have been reported at Granite Harbor and in the Kukri Hills.

The post-orogenic *Vida Granite* of the Victoria Intrusives intrudes Dais Granite and Olympus Granite-Gneiss in the western Asgard and Olympus mountains. The type locality is south of Lake Vida on the northern slope of the Olympus Range in Victoria Valley. The Vida Granite is a pink, hornblende-bearing, equigranular rock composed of orthoclase, oligoclase, quartz, biotite, and green hornblende with fine-grained interstitial quartz. Similar massive and unfoliated granitic intrusives have been reported from the valley of the Ferrar Glacier and from the coast of southern Victoria Land at Granite Harbor and Cape Irizar (Kurasawa et al. 1974).

All of the Wright and Victoria intrusives are cut by thin dikes of the *Vanda Lamprophyre and Porphyry*. At the type locality just east of Lake Vanda a swarm of these dikes intrudes the Dais and Vida granites and can be traced from there through Bull Pass into Victoria Valley. The lamprophyre is a dark aphanitic rock containing zoned plagioclase, green hornblende, chlorite, quartz, iron oxide, and accessory sphene and apatite. A typical porphyry dike at Bull Pass, about 6 m wide, contains phenocrysts of pink and white feldspar, greenish black hornblende, biotite, and quartz in a purplish aphanitic matrix.

The geology of Wright Valley mapped by McKelvey and Webb (1962) was extended by Allen and Gibson (1962) into the *Victoria Valley*. They described the Asgard Formation (Koettlitz Group) as a thick sequence of isoclinally folded marbles which are interbedded with layers of paragneiss, granulite, and quartzo-feldspathic schist. The metasedimentary rocks grade into Olympus Granite-Gneiss which passes gradationally into Dais Granite. The Asgard Formation (Koettlitz Group) and the Dais Granite are cut by the Vida Granite, and all of the basement rocks contain late-stage dikes of Vanda Lamprophyre and Porphyry.

The geology of *Taylor Valley* was initially examined by McKelvey and Webb (1959), Hamilton and Hayes (1960), and by Angino et al. (1960, 1962). Subsequently, Haskell et al. (1965a) published a map of the geology of Taylor Valley and described the metasediments of the Koettlitz Group which occur in four parallel north-trending belts, most prominent of which is the Middle-Taylor-Valley belt which is about 150 m wide. The metasediments of the Middle belt exposed along the south side of Taylor Valley consist of interbedded white marble, metaquartzite, magnesium-rich schist, calc-silicate hornfels, and quartzo-feldspathic schist. The mineral assemblages are consistent with the amphibolite facies and higher grades of regional metamorphism.

A second belt of Koettlitz-Group metasediments forms a south-plunging syncline in the *Nussbaum Riegel* which is a prominent topographic feature that projects from the Kukri Hills northward into Taylor Valley. According to Haskell et al. (1965a), the rocks of this feature consist of interbedded marble, metaquartzite, and quartz-labradorite-biotite schist. These rocks are correlative with the Asgard Formation (Koettlitz Group) of Wright and Victoria valleys (McKelvey and Webb 1962; Allen and Gibson 1962). In addition, Haskell et al. (1965a) correlated the rocks of Nussbaum Riegel with the basal part of the *Hobbs Formation* which occurs in the area between the Ferrar and the Koettlitz glaciers in Fig. 3.4. The structure and regional metamorphism of the metasedimentary rocks of Nussbaum Riegel were later described in great detail by Williams et al. (1971).

The metasedimentary rocks of the Koettlitz Group in Taylor Valley were intruded by several facies of the Granite Harbor Intrusives, including the highly foliated Olympus Granite-Gneiss, the Larsen Granodiorite which resembles the Dais Granite in Wright Valley, the Theseus Granodiorite, and the Irizar Granite. All of the different types of the Granite Harbor Intrusives and the metasedimentary rocks of the Koettlitz Group in Taylor Valley are cut by thin dikes of pegmatite, aplite, lamprophyre, porphyry, microdiorite, and ultramafic rocks.

The *Larsen Granodiorite* in Taylor Valley contains an orbicular phase located along the north side of the Taylor Glacier about 2.6 km from its terminus (Haskell et al. 1965a, Fig. 4). This occurrence was later investigated by Palmer et al. (1967) and by Dahl and Palmer (1981, 1983). Additional occurrences of orbicular textures were described by Allibone et al. (1993a).

A pluton of the post-tectonic *Irizar Granite*, exposed on Mt. Falconer (77°34'S, 163°08'E,) near the mouth of Taylor Valley, was studied by Ghent and Henderson (1968). These authors provided detailed petrographic descriptions of the various rock types exposed on Mt. Falconer and suggested that the Falconer pluton was originally emplaced at a depth of less than 8–10 km below the surface of the Earth. Parts of the pluton were exposed by erosion of the overlying rocks before sediment of the Beacon Supergroup was deposited on the Kukri Peneplain during the Early Devonian between 417 and 391 million years ago (IUGS 2002). McDougall and Ghent (1970) later reported K-Ar dates of biotite and hornblende from the Irizar Quartz Monzonite (adamellite) of the Mt. Falconer pluton, from the metasedimentary rocks of the Koettlitz Group, and from dikes that intruded the latter.

3.2 Koettlitz and Skelton Groups

The area between the Ferrar and the Skelton glaciers in Fig. 3.9 has been difficult to map because it is mountainous, snow-covered, and windy with occasional storms that can deposit up to 1.2 m of snow (Murphy et al. 1970; Flory et al. 1971; Rees et al. 1989). In spite of the active glaciation of most of this area, several ice-free valleys occur along the south side of the mountain range located between the Blue and Koettlitz glaciers (e.g., Garwood, Marshall, Miers, and Hidden valleys) which are identified on a map published by Bull (1962). The geology of this area was mapped by Blank et al. (1963) following Gunn and Warren (1962). In addition, Williams et al. (1971)

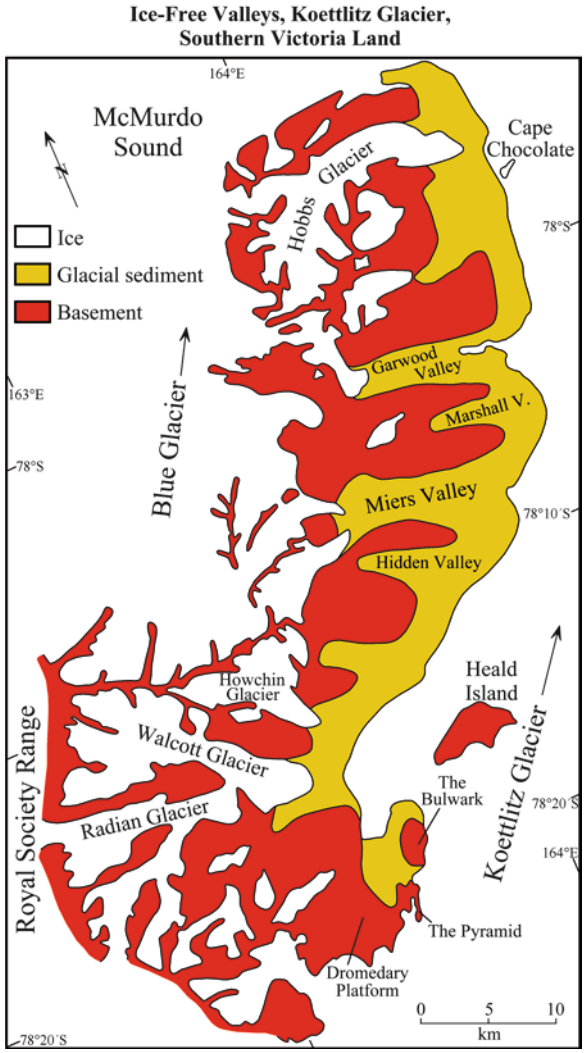

Fig. 3.9 The mountainous area between the Koettlitz and Blue glaciers is partially ice-free and exposes metasedimentary and metavolcanic rocks of the Koettlitz Group (Adapted from Bull 1962)

described the structure and metamorphism of metasedimentary basement rocks exposed in Garwood Valley and elsewhere in these ice-free valleys.

The multiply folded metasedimentary rocks that dominate the basement complex of this area were originally assigned to the Skelton Group by Gunn and Warren (1962). However, Grindley and Warren (1964) later placed only the low-grade metasedimentary rocks of the greenschist facies into the Skelton Group and assigned amphibolite-grade metasediments in the basement of southern Victoria Land to the Koettlitz Group.

Rocks of the Skelton Group are exposed on Teall Island, on both sides of the Skelton Glacier, and near Mt. Cocks between the Skelton and the Koettlitz Glaciers. Gunn and Warren (1962) divided the rocks of the Skelton Group into the upper *Teall Formation* and the underlying *Anthill Formation*, but Skinner (1982) later questioned the existence of the Teall Formation because the rocks at the type locality on Teall Island at the mouth of the Skelton Glacier resemble calc-silicate rocks that occur within the Anthill Formation. In place of the Teall Formation, Skinner (1982) defined the *Cocks Formation* based on metagraywacke and metavolcanic rocks that unconformably overlie the Anthill Formation (limestone) at Cocks Glacier (78°41'S, 162°00'E,).

The *Anthill Formation* is about 3,300 m thick (Stump 1995, p. 99) and consists of well-bedded white to grey limestone interbedded with lesser amounts of mudstone, siltstone, and quartzite. The limestone appears to be unfossiliferous. The metamorphic grade of the Anthill Formation increases from the greenschist facies on the south side of the Skelton Glacier to the amphibolite facies farther north between the Skelton and the Koettlitz glaciers.

The *Cocks Formation* contains a porphyritic pillow lava that was dated by Rowell et al. (1993) by means of the samarium-neodymium (Sm-Nd) method (Appendix 3.6.6). The rock yielded a Sm-Nd model date of 700–800 Ma, which indicates that the flow was extruded during the Neoproterozoic Era. The metamorphic grade of the Cocks Formation also increases in a northerly direction.

The variation of metamorphic grade of the metasedimentary basement rocks of southern Victoria Land has caused confusion because the distinction between of the Skelton and Koettlitz groups is based on metamorphic grade rather than on lithology or age of the rocks. Although the metasedimentary rocks of the ice-free valleys of southern Victoria Land were originally assigned to the Skelton Group, their metamorphic grade is more consistent with the Koettlitz Group which contains rocks in the amphibolite facies. Blank et al. (1963) defined five formations in the area between the Koettlitz and the Blue glaciers and assigned them to the Koettlitz Group with increasing stratigraphic age:

Hobbs Formation (youngest)
Salmon Marble
Garwood Lake Formation
Miers Marble
Marshall Formation (oldest)

However, Mortimer (1981) and Findlay et al. (1984) who also worked in the area did not agree with the stratigraphic sequence proposed by Blank et al. (1963). Mortimer (1981) concluded that the Salmon and Miers Marble were the same layer of rock and that the Garwood Lake and the Marshall Formation were also the same unit. Findlay et al. (1984) who remapped basement rocks throughout southern Victoria Land subdivided the Koettlitz Group into the Marshall Formation, the Salmon Marble, and the Hobbs Formation but did not place them in stratigraphic order.

In spite of the effort that has been made to identify mappable rock units in the Ferrar-Blue-Koettlitz-Skelton glaciers area, the relationship of the Skelton and Koettlitz groups remains in doubt. The only point of agreement among the investigators is that the rocks in both groups were deposited in a marine environment (Laird 1981). Moreover, both groups contain clastic metasediments, calc-silicates, marbles, conglomerates, volcanic rocks, and amphibolites. Therefore, the Skelton and Koettlitz groups could be regarded as a single complex of sedimentary and volcanic rocks of Neoproterozoic to Cambrian age whose metamorphic grade increases regionally from greenschist along the Skelton Glacier in the south to amphibolite in the Koettlitz-Blue Glacier area farther north. However, Stump (1995) recommended caution in the interpretation of the evidence which is still fragmentary and controversial (Rees et al. 1989).

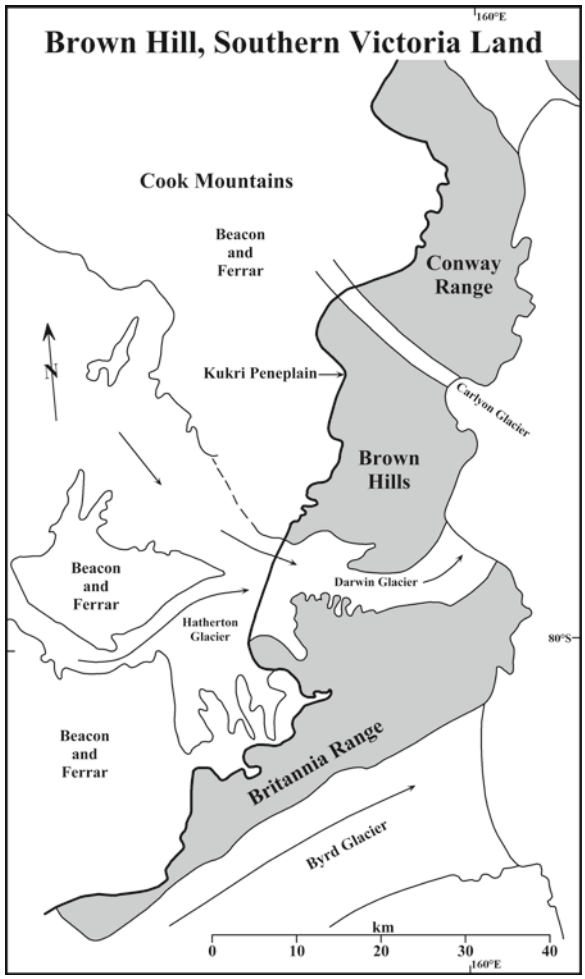

Fig. 3.10 The basement rocks that are exposed along the coast of the ice-free valleys of southern Victoria Land extend south into the Conway Range, the Brown Hills, and the Britannia Range. These rocks consist almost entirely of the Middle to Late Cambrian Granite Harbor Intrusives, which are subdivided into the Hope Granite, Skelton Granodiorite, Mt. Rich Granite, and the Carlyon Granodiorite. The older metasedimentary rocks of the Goldie Formation occur only in the form of inclusions within the granitic rocks of the Britannia Range (Adapted from Grindley and Laird 1969; Craddock 1969a)

3.3 Brown Hills

The basement rocks of southern Victoria Land in Fig. 3.10 extend south along the coast of the Ross Ice Shelf from the Skelton and Mullock glaciers to the Byrd Glacier. This segment of the Transantarctic Mountains contains the Conway Range, the Brown Hills, and the Britannia Range, all of which expose almost exclusively the granitic plutons of the Granite Harbor Intrusives (Grindley and Laird 1969). The granitic basement rocks of the Brown Hills in Fig. 3.11, which Encarnación and Grunow (1996) called the Brown Hills pluton, include the syntectonic Carlyon Granodiorite and the Mt. Rich Granite as well as the post-tectonic Hope Granite and dikes of leucocratic granite, pegmatite, lamprophyre, and meladiorite that cut the Carlyon and Mt. Rich plutons (Haskell et al. 1964, 1965b).

Metasedimentary rocks which are common in the ice-free valleys and in the Koettlitz-Skelton Glacier areas occur in the Brown Hills only as scattered inclusions within the Carlyon Granodiorite in the form of dark quartz-biotite-hornblende schist and light-colored metaquartzite. A large raft of metasediment, about 10,000 m^2 in area, occurs in the valley between the

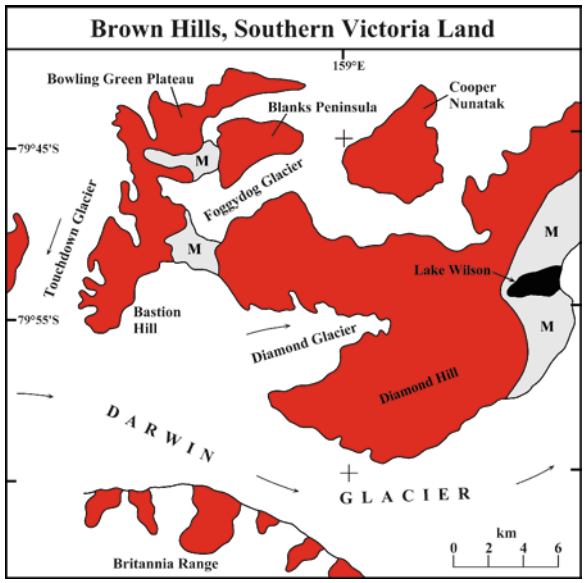

Fig. 3.11 The basement rocks exposed in the Brown Hills of southern Victoria Land consist almost exclusively of representatives of the Granite Harbor Intrusives (red) which were subdivided by Haskell et al. (1965b) into the synkinematic Carlyon Granodiorite and the Mt. Rich Granite followed by the post kinematic Hope Granite and a variety of dikes composed of leucocratic granite, pegmatite, lamprophyre, and meladiorite. Metasedimentary rocks consisting of quartz-biotite-hornblende schist occur only as scattered inclusions, the largest of which has an area of 10,000 m^2 and is located between the east end of Diamond Glacier and Lake Wilson (M = Moraine) (Adapted from Felder and Faure 1990, after Haskell et al. 1965b)

Fig. 3.12 Inclusion of metasedimentary rocks in the Granite Harbor Intrusives of the Brown Hills being investigated by Robert Felder during the 1978/79 Antarctic field season (Photo by G. Faure)

Diamond Glacier and Lake Wilson on the coast of the Ross Ice Shelf in Fig. 3.12. The strike of the metasedimentary rocks and the foliation of the Carlyon Granodiorite are parallel and the contact between them is gradational.

The Carlyon Granodiorite is medium to coarse grained, foliated to gneissic, and porphyritic in places. It grades into the Mt. Rich facies which is less foliated but more porphyritic than the Carlyon facies. Both intrusives are syntectonic and are composed of quartz, plagioclase, K-feldspar, biotite, hornblende, and sphene with accessory apatite, zircon, magnetite, and pyrite. The leucocratic dikes have higher concentrations of plagioclase and K-feldspar but lower concentrations of quartz and biotite than the Carlyon and Mt. Rich plutons and lack hornblende and sphene (Felder 1980). The average chemical analyses of the three major representatives of the Granite Harbor Intrusives published by Felder and Faure (1990) suggest that each was differentiated by fractional crystallization. However, differences in their initial $^{87}Sr/^{86}Sr$ ratios indicate that they are not the products of magmatic differentiation of a single parent magma.

A pluton composed of Hope Granite was mapped by Haskell et al. (1965b) on the Blanks Peninsula and the Bowling Green Plateau in Fig. 3.11. It is a fine-to-medium grained, equigranular, leucocratic granite composed of quartz, microcline, orthoclase, oligoclase, biotite, red garnet, and accessory chlorite. It resembles the Hope Granite described by Gunn and Walcott (1962) at the foot of Mt. Markham (82°51'S, 161°21'E,) located along the Lowery Glacier which is a southern tributary of the Nimrod Glacier (Section 5.2.3). The stratigraphic position of the Hope Granite is similar to that of the Vida Granite of the Victoria-Wright valleys and of the Irizar Granite in Taylor Valley. However, a genetic relationship among these post-kinematic granite plutons of southern Victoria Land has not yet been demonstrated.

3.4 Age Determinations

The geologic history of the basement rocks of southern Victoria Land started with the crystallization of crustal rocks of Gondwana which later became the source of sediment that was deposited along the passive paleo-Pacific margin of the continent. The sediment was subsequently folded and metamorphosed during the Ross Orogeny after the passive margin became a compressive subduction zone. During this active phase of the orogeny, the synkinematic plutons of the Granite Harbor Intrusives formed by crystallization of magma that originated by partial melting of accumulated sedimentary and volcanic rocks and by local recrystallization of the orogen (i.e., by granitization). After the main phase of the orogeny had ended, the magmatic activity continued with the intrusion of post-kinematic plutons and of various kinds of dikes of porphyry, lamprophyre, pegmatites, and mafic rocks. Although the sequence of events can be reconstructed by the interpretation of evidence in the field, the timing of the rock-forming events must be determined in the laboratory by radiogenic-isotope geochronometry (Faure and Mensing 2005). Summaries of the principal methods of dating igneous and metamorphic rocks are provided in Appendices 3.6.2–3.6.6.

Age determinations of rocks from the Transantarctic Mountains were included in several compilations of isotopic dates of Antarctic rocks. These compilations include, but are not necessarily limited to: Webb (1962), Picciotto and Coppez (1962, 1964a, b), Angino and Turner (1963), Ravich and Krylov (1964), Webb and Warren (1965), Craddock (1969b), Stuiver and Braziunas (1985), and others. Stuiver and Braziunas (1985) listed not only radiogenic-isotope dates, but also carbon-14 dates that record environmental processes during the most recent past extending to about 30,000 years before the present (BP).

3.4.1 K-Ar Dates

The first age determination of an Antarctic rock was reported by Goldich et al. (1958) who used the K-Ar method (Appendix 3.6.2) to date biotite from a sample of granite gneiss collected by P.N. Webb at Gneiss Point (77°24'S, 163°44'E,) on the coast of southern Victoria Land. Subsequently, additional K-Ar dates of biotite from the ice-free valleys were reported by Angino et al. (1962), Pearn et al. (1963), and McDougall and Ghent (1970). Although the numerical values of the decay constants of ^{40}K were changed after these reports were published, only the date reported by Goldich et al. (1958) is significantly altered when it is recalculated using the revised constants of Steiger and Jäger (1977).

The K-Ar dates of biotite in the basement rocks of Wright and Taylor valleys range from 425 to 520 million years (Ma) and have a slightly skewed but unimodal distribution in Fig. 3.13a. These dates record the time when the biotite cooled through its blocking temperature of 300 ± 25°C for radiogenic ^{40}Ar, whereas the blocking temperature of hornblende is 550 ± 25°C based on a compilation of data from the literature by Dallmeyer et al. (1981). Therefore, hornblende in a cooling body of rocks starts to retain radiogenic ^{40}Ar before biotite does, which causes K-Ar dates of hornblende to be *older* than K-Ar dates of biotite in the same body of rocks. The closure temperature of biotite (370 ± 20°C) reported by Berger and York (1981) agrees fairly well with that of Dallmeyer et al. (1981), but the closure temperature for hornblende (685 ± 55°C) of Berger and York (1981) is about 100° higher than that of Dallmeyer et al. (1981).

Although the K-Ar dates of biotites in the Granite Harbor Intrusives of the ice-free valleys in Fig. 3.13a post-date the time of crystallization of these rocks and form a "metamorphic veil" that obscures the crystallization age of the rocks, other methods of dating are available (to be discussed below) that do record the time of original crystallization of igneous and metamorphic rocks in spite of diffusion of radiogenic atoms during slow cooling of the rocks (i.e., the U-Pb method).

3.4.2 Rb-Sr Dates

Biotites in the granitic basement rocks of southern Victoria Land have also been dated by the Rb-Sr method which is based on the decay of naturally occurring radioactive ^{87}Rb to stable radiogenic ^{87}Sr (Appendix 3.6.3). The resulting Rb-Sr dates for biotite are just as sensitive to the loss of radiogenic ^{87}Sr during slow cooling as K-Ar dates of biotite. Therefore, Rb-Sr

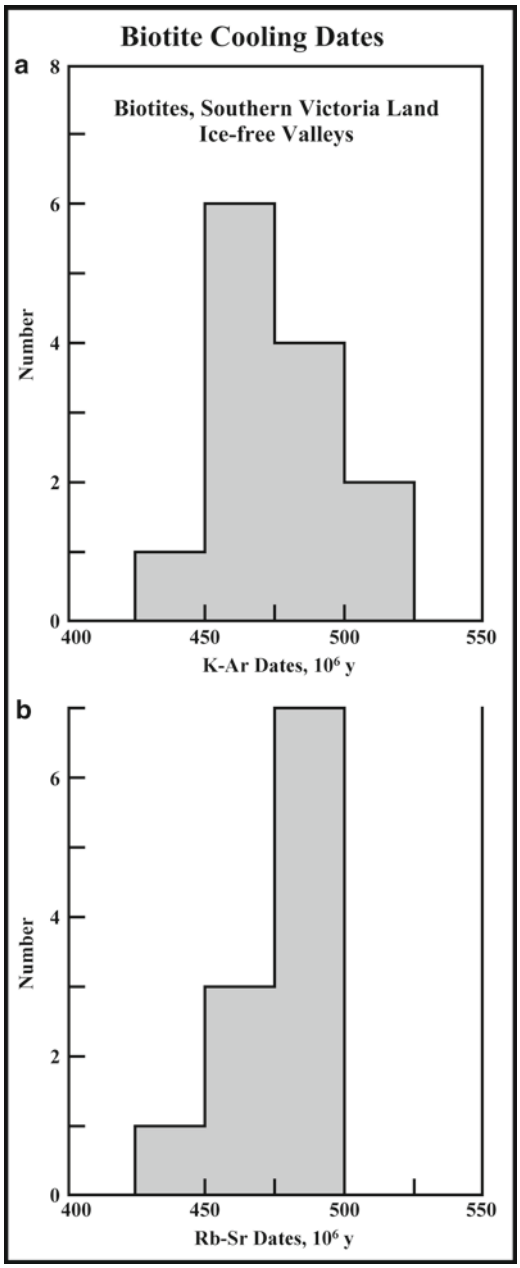

Fig. 3.13 (**a**) Histogram of K-Ar dates of biotite in the metasedimentary rocks (Asgard Formation, Koettlitz Group) as well as from the Granite Harbor Intrusives and late-stage mafic and lamprophyre dikes in Wright and Taylor Valley of southern Victoria Land. (Data from Goldich et al. 1958; Angino et al. 1962; Pearn et al. 1963; McDougall and Ghent 1970). (**b**) Histogram of Rb-Sr dates pf biotite in rocks of the basement complex described above. All dates were recalculated to $\lambda = 1.42 \times 10^{-11}$ year^{-1} for the decay constant of ^{87}Rb (Data from Deutsch and Webb 1964)

dates of biotite also record the time when plutonic igneous and high-grade metamorphic rocks cooled through the blocking temperature of Sr in biotite. In addition, Rb-Sr dates of single specimens of rocks and minerals (so-called "model dates") are based on assumed values of the initial $^{87}Sr/^{86}Sr$ ratio as explained in Appendix 3.6.3 and by Faure and Mensing (2005). This requirement does not apply to the calculation of K-Ar dates because the number of ^{40}Ar atoms that were incorporated into biotite or hornblende at the time these minerals crystallized from a magma is assumed to be zero.

The Rb-Sr dates of biotite extracted from rocks of the Asgard Formation (Koettlitz Group) and from the granitic intrusives in the ice-free valleys reported by Deutsch and Webb (1964) have a unimodal but skewed distribution in Fig. 3.13b. One biotite sample from the Koettlitz Group analyzed by those authors yielded an anomalously low Rb-Sr date of only 334 Ma (recalculated to $\lambda = 1.42 \times 10^{-11}$ year^{-1} for ^{87}Rb). Deutsch and Webb (1964) reported that this sample was collected "a few hundred feet" from a dolerite dike of the Middle Jurassic Ferrar Group and probably lost radiogenic ^{87}Sr as a result of heating during contact metamorphism. When this date is excluded, the Rb-Sr dates of biotite reported by Deutsch and Webb (1964) range from 425 to 500 million years and do not differ significantly from the K-Ar dates of biotites in Fig. 3.13a which were measured on a different set of samples collected in Wright and Taylor valleys.

A mixture of biotite and hornblende from a post-kinematic *porphyry dike* dated by Deutsch and Webb (1964) yielded a Rb-Sr date of 467 ± 15 Ma (recalculated to $\lambda = 1.42 \times 10^{-11}$ year^{-1}). This Middle Ordovician date may approach the crystallization age of this rock because the porphyry dikes in the basement of southern Victoria Land are thin (less than 1 m) and therefore cooled more rapidly than the much more voluminous Granite Harbor Intrusives (e.g., Olympus, Dais, Theseus, Vida, and Irizar).

Deutsch and Webb (1964) also reported an anomalously *old date* of 922 ± 80 Ma for a feldspar concentrate and 979 ± 80 Ma for a whole-rock sample from the same porphyry dike. These dates taken at face value suggested that this porphyry dike had crystallized about 1,000 million years ago, which implied that the basement rocks in the ice-free valleys had

formed in Precambrian time more than 1,000 million years ago. In order to test this conclusion, Jones and Faure (1967) dated two porphyry dikes in Wright Valley by the Rb-Sr isochron method. The results in Fig. 3.14 yielded a well-constrained date of 470 ± 7 Ma (recalculated to $\lambda = 1.42 \times 10^{-11}$ year^{-1}). This date is a reliable determination of the age of the porphyry dikes in Wright Valley and confirms that their age is Middle Ordovician rather than Neoproterozoic.

The whole-rock Rb-Sr dates of the granitic intrusives in the ice-free valleys of southern Victoria Land in Table 3.3 range from 478 ± 4 to 490 ± 14 Ma (Allibone et al. 1993a; Faure et al. 1974). A well-defined Rb-Sr isochron for leucocratic granite dikes in the Brown Hills of 484 ± 6 Ma also fits in that range (Felder and Faure 1990). Several other whole-rock Rb-Sr isochron dates listed in Table 3.3 have large uncertainties caused by scatter of the initial $^{87}Sr/^{86}Sr$ ratios within individual plutons. The dates measured by Stuckless and Erickson (1975), Graham and Palmer (1987), and Allibone et al. (1993a) by a combination of whole-rock samples and constituent minerals range from 493 ± 17 Ma (Bonney pluton, Kukri Hills) to 472 ± 15 Ma (hornblende-biotite orthogneiss, Wright Valley). Two dates in this set are marginally younger (452 and 459 Ma, quartz monzonite, Granite Harbor) perhaps because biotite in these rocks lost radiogenic ^{87}Sr.

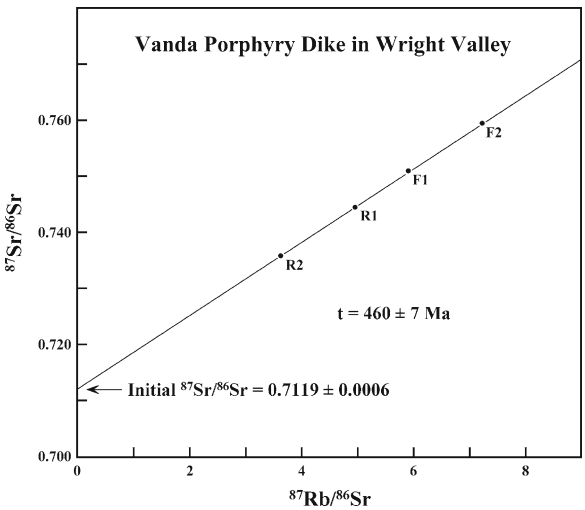

Fig. 3.14 Rb-Sr isochron defined by whole-rock samples of two Vanda Porphyry dikes (R1 and R2) and K-feldspar concentrates (F1 and F2). The date of 460 ± 7 Ma is the crystallization age of these dikes which were intruded into the metasedimentary rocks of the Asgard Formation, and into the plutonic igneous rocks of the Granite Harbor Intrusives in Wright Valley during the Middle Ordovician Epoch after the Ross Orogeny (Plotted from data by Jones and Faure 1967)

The slopes of Rb-Sr mineral isochrons are controlled primarily by biotite which has much higher $^{87}Rr/^{86}Sr$ ratios than K-feldspar, hornblende, or whole-rock samples (e.g., $^{87}Rb/^{86}Sr$ = 24.383 to 122.491). Consequently, the statistical precision of such dates is improved by inclusion of biotite on the isochron, but the dates calculated from the slope of the isochrons may be lowered if some of the accumulated radiogenic ^{87}Sr was lost from biotite during slow cooling and/or reheating of the rocks after crystallization from magma. Therefore, Rb-Sr isochron dates based on whole-rock samples and constituent minerals (e.g., biotite) need to be evaluated cautiously.

Most of the granitic rocks in southern Victoria Land that have been dated by the Rb-Sr whole-rock or whole-rock/mineral isochron methods in Table 3.3 have elevated initial $^{87}Sr/^{86}Sr$ ratios ranging from 0.70861 ± 0.00010 to 0.7121 ± 0.0011 compared to values between 0.7035 and 0.7045 for basalt that originated by decompression melting in the subcrustal mantle of the Earth (Faure 2001). Therefore, the granitic magmas that intruded the Ross orogen in southern Victoria Land and elsewhere in the Transantarctic Mountains contained *excess* radiogenic ^{87}Sr of crustal origin. Such magmas may form by partial melting during orogenic deformation and metamorphism of volcano-sedimentary complexes.

The age determinations of biotite and of whole-rock samples of the granite intrusives of southern Victoria Land reveal the timing of significant events in the evolution of the Ross orogen in this area. However, all of these dates *post-date* the deposition of the sediment along the paleo-Pacific coast of Gondwana. Adams and Whitla (1991) attempted to fill this gap in the history of the Ross orogen by using the whole-rock Rb-Sr method to date samples of the Asgard Formation (Koettlitz Group) collected in Wright and Victoria valleys. The time of deposition of clastic sedimentary rocks is difficult to determine by this method because the initial $^{87}Sr/^{86}Sr$ ratios of whole-rock samples depend on their lithologic composition and provenance. Therefore, whole-rock samples of sedimentary rocks in many cases scatter above and below Rb-Sr isochrons, which increases the uncertainty of dates derived from them and may introduce systematic errors. Adams and Whitla (1991) assumed that the isotopic composition of strontium in different lithologies

Table 3.3 Summary of radiogenic-isotope dates of plutonic igneous and metasedimentary rocks of the basement rocks of southern Victoria Land

Geologic unit	Date, Ma	$(^{87}Sr/^{86}Sr)_i$	References
Whole-rock Rb-Sr isochrons			
Marble, Asgard Fm., Koettlitz Gp.	840 ± 30	0.7081	1
Quartz-feldspar schist, Asgard Fm.	~670	0.707–0.713	1
Mica schist, Asgard Fm.	>615 ± 15	0.727	1
Olympus Granite Gneiss, Wright Valley	488 ± 43	0.7109 ± 0.0007	2
Vida Granite and Vanda Porphyry	471 ± 44	0.7104 ± 0.0008	2
Vanda Porphyry dikes	460 ± 7	0.7119 ± 0.0006	3
Harker pluton, St. Johns Range	478 ± 4	0.70952 ± 0.00012	4
St. Johns pluton, St. Johns Range	490 ± 14	0.70881 ± 0.00010	4
Granite, Lion Island, Cape Archer, Gregory Island	478 ± 35	0.70870 ± 0.00084	4
Carylon Granodiorite, Brown Hills	568 ± 9	0.7122 ± 0.00015	10
Mt. Rich Granite, Brown Hills	593 ± 238	0.7084 ± 0.0014	10
Leucocratic Granite dikes, Brown Hills	484 ± 6	0.7119 ± 0.0006	10
Whole-rock plus mineral Rb-Sr isochrons			
Vida Granite, Lake Vida	476 ± 14	0.7098 ± 0.0007	5
Avalanche Bay 77°01'S, 162°44'E,	452 ± 6	0.70892 ± 0.00005	6
Couloir Cliffs 77°01'S, 162°44'E,	459 ± 4	0.70903 ± 0.00056	6
Robertson Ridge 77°24'S, 162°12'E,	480 ± 14	0.70879 ± 0.00010	6
Hornblende-biotite orthogneiss, Wright Valley	472 ± 15	0.70861 ± 0.00010	4
Bonney pluton, Kukri Hills	493 ± 17	0.70893 ± 0.00008	4
Bonney pluton, Cathedral Rocks	479 ± 15	0.71016 ± 0.00013	4
$^{40}Ar/^{39}Ar$ plateau dates			
Biotite, CarylonGranodiorite, Brown Hills	513 ± 6, 504 ± 5, 508 ± 5		10
Hornblende, Carylon Granodiorite, Brown Hills	515 ± 6, 534 ± 6		10
Biotite, Mt. Rich Granite, Brown Hills	515 ± 5		10
$^{40}Ar/^{39}Ar$ total-gas release dates			
Biotite, Carylon Granodiorite, Brown Hills	476–510		10
Biotite, Mt. Rich Granite, Brown Hills	486–519		10
Hornblende, Carlyon Granodiorite, Brown Hills	531		10
U-Pb dates of zircon			
Couloir Cliffs, Granite Harbor	498 ± 4		7
Porphyry dike, Wright Valley	484 ± 7		7
Bonney pluton, Miers Ridge	505 ± 2		7
Granite, Cocks-Skelton Glacier	551 ± 4		7
Hornblende-biotite granite, Brown Hills	515 ± 8		7
Vida Granite, zircon	447 ± 34		8
Olympus Granite-Gneiss, zircon	462 ± 6		8
Olympus Granite-Gneiss, provenance	2554 ± 330		8
Olympus Granite-Gneiss	610 Upper intercept		9
Quartz syenite, Skelton-Cocks Glacier	551 ± 4		11
Sm-Nd model date			
Basalt, Cocks Fm., Skelton Glacier	809 ± 10		11

1 Adams and Whitla (1991); 2. Faure et al. (1974); 3. Jones and Faure (1967); 4. Allibone et al. (1993a); 5. Stuckless and Erickson (1975); 6. Graham and Palmer (1987) modified by Allibone et al. (1993a); 7. Encarnación and Grunow (1996); 8. Vocke and Hanson (1981); 9. Deutsch and Grőgler (1966); 10. Felder and Faure (1980, 1990); 11. Rowell et al. (1993) recalculated by Faure and Mensing.

of the Asgard Formation was homogenized during regional metamorphism and that the $^{87}Sr/^{86}Sr$ ratios of the pelitic layers had approached the values that existed in the limestone layers. However, the results do not support this assumption.

The measured $^{87}Rb/^{86}Sr$ ratios of the 37 rock samples analyzed by Adams and Whitla (1991) ranged widely from 0.086 to 11.88 depending on the presence of biotite, which is the principal Rb-bearing mineral in these rocks followed by K-feldspar. In addition to

quartz-biotite-feldspar schists, the analyzed rock samples included marbles, amphibolites, and biotite-hornblende schists. The $^{87}Sr/^{86}Sr$ and $^{87}Rb/^{86}Sr$ ratios of the samples analyzed by Adams and Whitla (1991) form one coherent array (not shown) with the exception of two biotite schist samples from Wright Valley that have high $^{87}Rb/^{86}Sr$ ratios of >4.0. Adams and Whitla (1991) grouped these data on the basis of their lithologic composition and calculated separate Rb-Sr isochron dates for each group ($\lambda = 1.42 \times 10^{-11}$ year^{-1}): Mica schist, >615 ± 15 Ma; Quartz-feldspar schist, ~670 Ma; Marbles, 840 ± 30 Ma.

The authors concluded that the mica schists were regionally metamorphosed prior to 615 ± 15 Ma and that the isotopic composition of strontium in the quartz-feldspar schists was incompletely homogenized during a preceding event at about 670 Ma. A well-defined isochron of three samples of impure marble in Fig. 3.15 records the time when these rocks were deposited at 840 ± 30 Ma during the Neoproterozoic Era. The initial ratio of the marbles (0.7081) is higher than values of this ratio for unaltered marine carbonate rocks at 840 ± 30 Ma (Faure and Mensing 2005, p. 450). The chemical analysis published by Adams and Whitla (1991) for one of the marble samples suggest that the apparent enrichment of the marbles in ^{87}Sr is probably attributable to the presence of Sr-bearing impurities that were included in the carbonate minerals at the time of deposition (e.g., illite).

3.4.3 $^{40}Ar/^{39}Ar$ Dates

Felder and Faure (1990) dated biotite and hornblende in the granitic basement rocks of the Brown Hills by the $^{40}Ar/^{39}Ar$ method (Faure and Mensing 2005). This method is superior to the conventional K-Ar method because it is capable of reliably dating minerals even when they have lost some of the radiogenic ^{40}Ar that formed by the decay of ^{40}K (Appendix 3.6.4). The step-wise release $^{40}Ar/^{39}Ar$ dates of three biotites in the Carlyon Granodiorite reported by Felder and Faure (1990) are tightly clustered between 504 ± 5 and 513 ± 5 Ma with a mean of 508 ± 5 Ma, whereas two hornblendes in the Carlyon Granodiorite have partial release dates of 515 ± 6 and 534 ± 6 Ma. The older of the two hornblendes (534 ± 6 Ma) has a well developed partial-release plateau in Fig. 3.16 that represents the time when this mineral cooled through its blocking temperature for radiogenic ^{40}Ar. The other hornblende fraction contained biotite which explains its lower partial-release date (i.e., 515 ± 6 Ma). Therefore, the Carlyon Granodiorite cooled through the blocking temperature of hornblende (550 ± 25°C) at 534 ± 6 Ma and reached the blocking temperature of biotite (300 ± 25°C) at about 508 ± 5 Ma which yields a cooling rate of 9.6°C/Ma. These age determinations suggest that the crystallization age of the Carlyon Granodiorite and of the Mt. Rich Granite is more than 534 ± 6 Ma, which is in satisfactory agreement with the whole-rock Rb-Sr

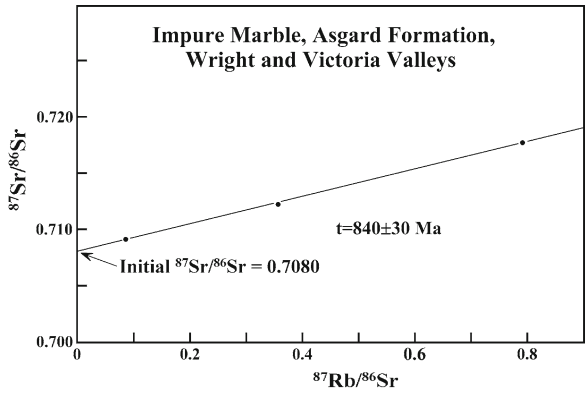

Fig. 3.15 Three whole-rock samples of marble in the Asgard Formation (Koettlitz Group) define a straight line on the Rb-Sr isochron diagram that yields a date of 840 ± 30 Ma and an initial $^{87}Sr/^{86}Sr$ ratio of 0.7080. Date and initial $^{87}Sr/^{86}Sr$ ratio calculated by Adams and Whitla (1991) from their own measurements.

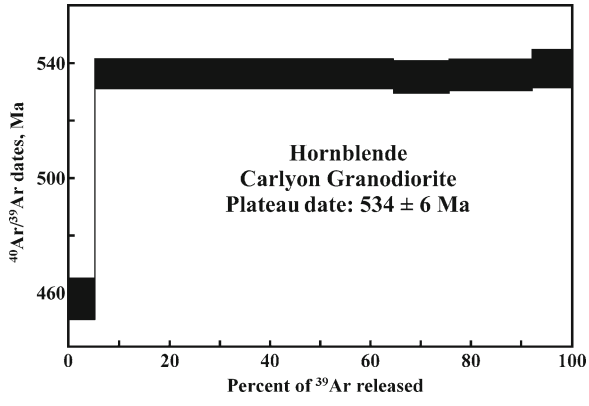

Fig. 3.16 The $^{40}Ar/^{39}Ar$ ratios of argon released by step-wise heating of a powdered sample of neutron-irradiated hornblende were used to calculate a series of dates which define a plateau at 534 ± 6 Ma. This date is a reliable estimate of the crystallization age of the Carlyon Granodiorite in the Brown Hills, southern Victoria Land (Replotted from data by Felder and Faure 1990)

date of the Carlyon Granodiorite (568 ± 34 Ma) listed in Table 3.3.

Felder and Faure (1990) also reported total-gas dates of biotites and hornblende from the Carlyon Granodiorite (biotite, 501–510 Ma; hornblende, 531 Ma) and from the Mt. Rich Granite (biotite, 486–519 Ma). These dates are equivalent to conventional K-Ar dates. Nevertheless, the total gas date of the hornblende (531 Ma) is indistinguishable from the partial-release plateau date (534 ± 6 Ma) of the same sample.

More recently, Encarnación and Grunow (1996) reported a U-Pb date of 515 ± 8 Ma for zircon in the equigranular and unfoliated granite of the Cooper Nunatak in the Brown Hills (see below). This date is compatible with the $^{40}Ar/^{39}Ar$ dates of biotites and hornblende reported by Felder and Faure (1990) and further constrains the time of intrusion and crystallization of the granite plutons in the Brown Hills.

3.4.4 U-Pb Dates

The U,Th-Pb methods of dating igneous and metamorphic rocks is based on the decay of the isotopes of uranium and thorium to stable isotopes of lead: $^{238}U \rightarrow ^{206}Pb$; $^{235}U \rightarrow ^{207}Pb$; $^{232}Th \rightarrow ^{208}Pb$ in U, Th-bearing minerals such as zircon, sphene, apatite, or even rutile (Appendix 3.6.5). This method was used by Deutsch and Grőgler (1966) to date zircon grains extracted from a sample of Olympus Granite-Gneiss collected at 77°25' and 162°05'E, along the south shore of Lake Vida in Victoria Valley. The dates calculated by the authors for three zircon size-fractions are *discordant*, which implies that the zircons lost varying amounts of radiogenic lead or gained uranium and/or thorium (Faure and Mensing 2005). An interpretation of these data on a *concordia diagram* (Appendix 3.6.5) by the authors indicates that the zircons crystallized at about 610 Ma (or lost all pre-existing radiogenic lead) and subsequently lost varying amounts of radiogenic lead right up to the present. A later re-interpretation of the data by Vocke and Hanson (1981) yielded an upper-intercept date of 638 ± 92 Ma on a U-Pb concordia diagram and a lower-intercept date of 200 ± 193 Ma which is indistinguishable from zero.

Vocke and Hanson (1981) also dated zircons which they extracted from samples of the Vida Granite and the Olympus Granite-Gneiss in core 6 recovered by the Dry Valley Drilling Project (DVDP) at Lake Vida in Victoria Valley. An examination of the zircon grains in the Olympus Granite-Gneiss by cathodoluminescence revealed that these grains contain old cores with more recent overgrowths. Therefore, the data points representing different size-fractions define a chord on the concordia diagram in Fig. 3.17 that has an upper intercept at 2554 ± 330 Ma and a lower intercept at 462 ± 6 Ma. The most plausible interpretation of these dates in the context of the geology of southern Victoria Land is that the zircon cores are detrital grains that originally crystallized in Late Archean/Paleoproterozoic time. Accordingly, the upper-intercept date is the time of crystallization of the zircons in the *source area* from which they were liberated by erosion (i.e., it is the age of provenance). After deposition along the passive paleo-Pacific margin of Gondwana, the zircon grains

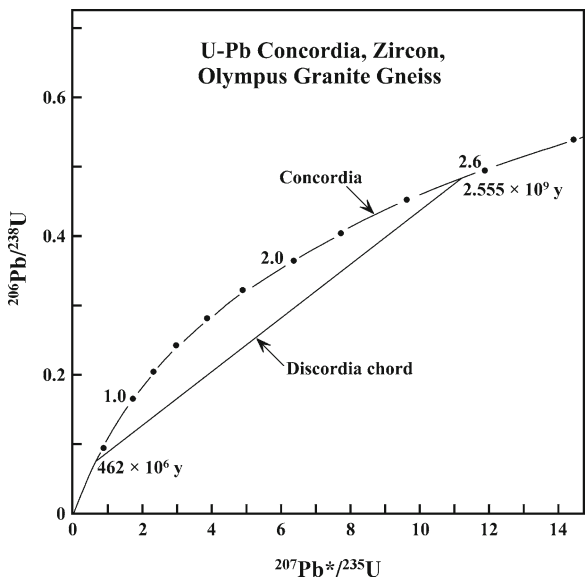

Fig. 3.17 The U-Pb concordia curve is plotted by solving Eqs. 3.16 and 3.17 for the same value of t in order to obtain the $^{206}Pb^*/^{238}U$ and $^{207}Pb^*/^{235}U$ ratios of points that represent concordant U-bearing minerals (see Faure and Mensing 2005, Table 10.3, p. 220). The discordant zircon crystals of the Olympus Granite-Gneiss analyzed by Vocke and Hanson (1981) define the discordia chord which intersects concordia at two points. The coordinates of these two points yield concordant dates by solving Eq. 3.18 or 3.19 (or both). Lower intercept, t = 462 ± 6 Ma; upper intercept, t = 2555 ± 330 Ma. The upper intercept yields the original crystallization age of the provenance of the zircon. The lower intercept is the time that has elapsed since the abraded zircon grains acquired fresh overgrowths during the Ross Orogeny. A more comprehensive interpretation was provided by Vocke and Hanson (1981) and by Vocke et al. (1978)

developed overgrowths at 462 ± 6 Ma by regional metamorphism of the sediment during the Ross Orogeny. Although the zircons analyzed by Vocke and Hanson (1981) have old cores, those of Deutsch and Grőgler (1966) do not, even though both originated from the Olympus Granite-Gneiss in Victoria Valley. A more comprehensives study of zircons in the granitic plutons of the ice-free valley could shed light on the provenance of the zircons and on the age of the plutons in which they now reside.

Different size fractions of the zircons extracted by Vocke and Hanson (1981) from the *Vida Granite* in DVDP6 define a chord that intersects the concordia curve at 447 ± 34 Ma and at 0 Ma. The upper intercept is the crystallization age of zircon in the Vida Granite and the lower intercept (0 Ma) indicates that the zircons may have been losing radiogenic lead by continuous diffusion as a result of chemical weathering.

Size-fractions of zircon extracted from a pluton of unfoliated quartz diorite which intrudes the intensely folded metasedimentary rocks of the *Anthill and Cocks formations* in the Skelton Glacier-Cocks Glacier area at 78°39' and 161°00'E, were dated by Rowell et al. (1993) by the U-Pb method. The data define a chord that intersects concordia at a point that corresponds to a well-constrained date of 551 ± 4 Ma. Zircon from a second pluton, composed of granite and located only 1 km from the quartz-diorite pluton, yielded an identical date of 551 ± 4 Ma (Encarnación and Grunow 1996). This date not only establishes the age of the two plutons, but also sets a lower limit to the time of deposition and deformation of the metasedimentary rocks that were intruded by these plutons.

3.4.5 Sm-Nd Dates

The most reliable way to determine the depositional age of unfossiliferous sedimentary (or metasedimentary) rocks is to date mafic volcanic rocks that may be interbedded with them. The Asgard Formation (Koettlitz Group) of the Wright and Victoria valleys as well as the Cocks Formation of the Skelton Glacier area contain *interbedded basalt*. The volcanic rocks in the *Asgard Formation* (Koettlitz Group) of Wright and Victoria valleys are represented by amphibolite and hornblende schist both of which have low initial $^{87}Sr/^{86}Sr$ ratios of 0.7032 ± 0.0002 and 0.70475 ± 0.00025, respectively (Adams and Whitla 1991). The *Cocks Formation* in the Skelton-Glacier area contains pillow basalts which were analyzed by Rowell et al. (1993) for dating by the Sm-Nd method (Appendix 3.6.6).

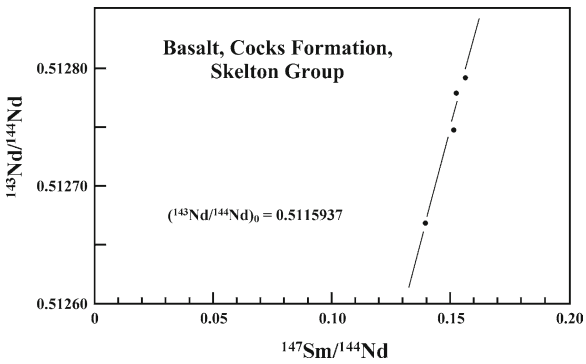

Fig. 3.18 The $^{147}Sm/^{144}Nd$ and $^{143}Nd/^{144}Nd$ ratios of a whole-rock sample and magnetic fractions of a pillow basalt in the Cocks Formation, Skelton Glacier area, define a straight line that was used to determine the initial $^{143}Nd/^{144}Nd$ ratio of this rock. The value was used in Appendix 3.6.6 to calculate a model date of 809 Ma based on the isotopic evolution of neodymium in CHUR (Plotted from data by Rowell et al. 1993)

We used the $^{143}Nd/^{144}Nd$ and $^{147}Sm/^{144}Nd$ ratios of one whole-rock basalt sample and three magnetic splits reported by Rowell et al. (1993) to determine their initial $^{143}Nd/^{144}Nd$ ratio by means of the Sm-Nd isochron diagram in Fig. 3.18. An unweighted least-squares regression of the data yields a value of 0.511594 for the initial $^{143}Nd/^{144}Nd$ ratio which we used to calculate the time in the past when the $^{143}Nd/^{144}Nd$ ratio of the chondritic uniform reservoir (CHUR) of the Earth in Fig. 3.19 had this value. The resulting Sm-Nd model date of 809 ± 10 Ma is similar to the date obtained by Rowell et al. (1993) who reported t = 700 to 800 Ma.

The Sm-Nd model date calculated above is the time when the pillow basalt in the *Cocks Formation* could have been erupted and was subsequently buried by sediment. If this conjecture is correct, then the age of the basalt is equal to the time of deposition of the sediment of the Cocks Formation. The Sm-Nd isotope systematics of mafic volcanic rocks are sufficiently robust to remain undisturbed by structural deformation and regional metamorphism as exemplified by volcanic rocks of Archean age (e.g., komatiite flows, Onverwacht Group, South Africa dated by Hamilton et al. 1979).

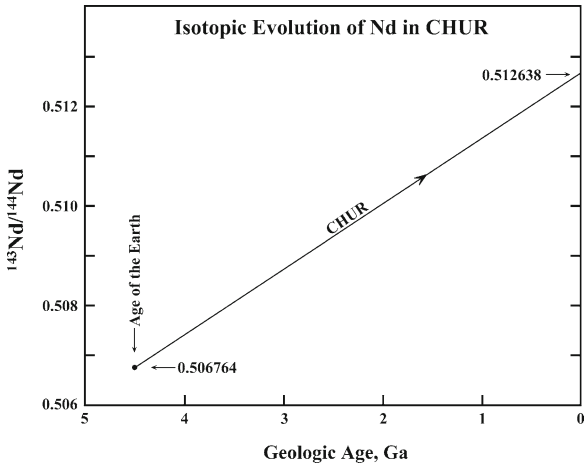

Fig. 3.19 The $^{143}Nd/^{144}Nd$ ratio of neodymium in the Chondritic Uniform Reservoir (CHUR) which represents the mantle of the Earth, increases as a function of time because of the alpha-decay of naturally-occurring radioactive ^{147}Sm (samarium). The initial $^{143}Nd/^{144}Nd$ ratio of CHUR at t = 4.5 × 10^9 years was 0.50674 and the present value of this ratio at t = 0 years is 0.512638

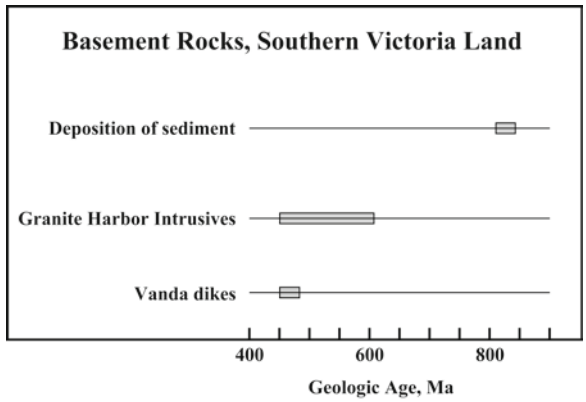

Fig. 3.20 The isotopic age determinations reviewed in this chapter were used to reconstruct the geologic history of the basement rocks of the Transantarctic Mountains in southern Victoria Land

3.5 Geologic History of Southern Victoria Land

The age determinations compiled in Table 3.3 can be used to reconstruct the geologic history of the Ross Orogen in southern Victoria Land with due regard to several self-evident considerations:

1. The geologic processes by means of which the rocks of the orogen originated acted slowly in the course of tens of millions of years.
2. The geologic processes did not occur everywhere at the same time but acted randomly in terms of time and space.
3. The radiogenic isotope systematics of K-Ar, Rb-Sr, and U-Pb were altered during tectonic deformation of sedimentary rocks, during slow cooling of granitic plutons and of high-grade metamorphic complexes.
4. The alteration of the isotope systematics occurred not only at high temperature and pressure at depth in the crust, but also at low temperature and pressure at shallow depth during the erosion of overlying strata of the Ross Mountains which were reduced to the Kukri Peneplain.
5. The sedimentary rocks were originally saturated with water which was squeezed out during tectonic deformation and regional metamorphism. The resulting flux of aqueous fluids toward the surface of the Earth contributed to the loss of radiogenic isotopes from minerals at depth in the crust.

The geologic history of the Ross Orogen in Fig. 3.20 started when the supercontinent Rodinia split into Gondwana and Laurentia which subsequently drifted apart. The resulting passive rift-margin of Gondwana permitted sediment and interbedded basalt lava to accumulate off-shore. The interval of time during which sediment and pillow lavas accumulated in the ocean off the passive margin of Gondwana is indicated by the whole-rock Rb-Sr isochron date of 840 ± 30 Ma for marbles in Wright and Victoria Valleys (Adams and Whitla 1991). Another date from that time period is the model Sm-Nd date of pillow basalt in the Cocks Formation of the Skelton-Glacier area (809 ± 10 Ma) based on data by Rowell et al. (1993). Consequently, the break-up of Rodinia occurred *prior* to these dates.

The clastic sediment that was deposited along the passive rift margin of Gondwana originated from the source regions that had crystallized in Neoarchean/Paleoproterozoic time at about 2554 ± 330 Ma (Vocke and Hanson 1981). Some time after 809 ± 10 Ma, the passive rift margin of Gondwana was transformed into a compressive subduction zone following unspecified changes in the pattern of convection of the mantle beneath the paleo-Pacific Ocean. As a result, the sedimentary-volcanic complex was compressed against the Gondwana craton, dewatered, extensively folded, and heated, which caused regional metamorphism that

ranged from the greenschist to the amphibolite facies. Parts of the sedimentary-volcanic complex may have been subducted beneath the continental crust of Gondwana, which caused uplift of the continental margin. The intensity of regional metamorphism of the wet sediment was sufficient to cause large volumes of granitic magma to form by partial melting which intruded the overlying rocks while they were being deformed.

The resulting batholiths and plutons of the Granite Harbor Intrusives crystallized as they were being deformed by tectonic stress. The magmatic activity started during the latest Neoproterozoic to Early Cambrian time as exemplified by the Carlyon granodiorite/Mt. Rich granite of the Brown Hills which was dated by a whole-rock Rb-Sr isochron at 568 ± 54 Ma, by a $^{40}Ar/^{39}Ar$ plateau date of hornblende of 534 ± 6 Ma, and by a total Ar-release date of 531 Ma (Felder and Faure 1990). In addition, Encarnación and Grunow (1996) reported a U-Pb concordia date of zircon of 551 ± 4 Ma for a granite in the Cocks-Skelton Glacier area, and Rowell et al. (1993) obtained an identical U-Pb zircon date for a nearby quartz-syenite pluton. Deutsch and Grőgler (1966) reported an even older U-Pb concordia date of 638 ± 92 Ma for zircon in the Olympus Granite-Gneiss in Victoria Valley (recalculated by Vocke and Hanson 1981).

The magmatic activity continued for several tens of millions of years until it ended at about 460 ± 7 Ma with the intrusion of the Vanda Porphyry dikes in Wright Valley (Jones and Faure 1967). At this time in the geologic history of southern Victoria Land, a chain of high mountains existed along the former rift margin of Gondwana. The so-called Ross Mountains were subsequently eroded to form the Kukri Peneplain on which the sandstones and other clastic sedimentary rocks of the Beacon Supergroup were deposited starting at about 415 Ma in Early Devonian time.

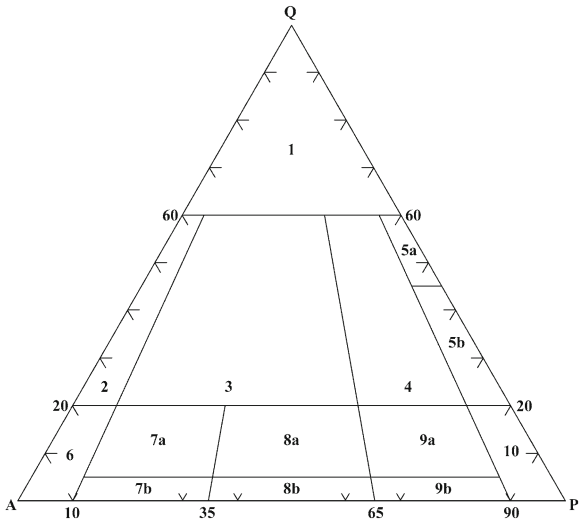

Fig. 3.21 The classification of plutonic igneous rocks by Streckeisen (1967, 1976) is based on the modal abundances of quartz (Q), alkali feldspar (including albite, An < 5%) (A), and plagioclase (An > 5%) (P). The fields have been numbered in order to identify the rock types that correspond to them: 1. quartz, 2. alkali granite, 3. granite, 4. granodiorite, 5a. quartz diorite (trondhjemite), 5b. quartz diorite (tonalite), 6. alkali syenite, 7a. quartz syenite, 7b. syenite, 8a. quartz monzonite (adamellite), 8b. monzonite, 9a. monzodiorite, 9b. monzogabbro, 10. diorite/gabbro (Adapted from Streckeisen 1967)

3.6 Appendices

3.6.1 Classification of Plutonic Rocks of Granitic Composition

Plutonic rocks of "granitic" composition are classified on the basis of the *modal* abundances of quartz, alkali feldspar including albite (An 0–5%), and plagioclase (An > 5%). The resulting triangular Q-A-P diagram was subdivided by Streckeisen (1967, 1976) into fields in Fig. 3.21 and numbered consecutively from 1 to 10. The plutonic rocks that occupy each of these fields are identified in the caption to Fig. 3.21. Four of the principal fields are subdivided as indicated by the letters *a* and *b*. For example, 7a contains quartz syenites while 7b is occupied by regular syenites. Streckeisen's classification has been widely used to classify granitic rocks of the Granite Harbor Intrusives in the Transantarctic Mountains.

3.6.2 K-Ar Method

Potassium has three naturally occurring isotopes:

$$^{39}_{19}K = 93.26\%, \; ^{19}_{40}K = 0.0117\%, \text{and } ^{19}_{41}K = 6.73\%.$$

Potassium-40 is radioactive and decays by branched decay to ^{40}Ar and to ^{40}Ca. The number of radiogenic decay products that accumulate as a function of time

is expressed by an equation derived from the Law of Radioactivity (Faure and Mensing 2005).

$$^{40}\mathrm{Ar}^{*} + {}^{40}\mathrm{Ca}^{*} = {}^{40}\mathrm{K}\left(e^{\lambda t} - 1\right) \tag{3.1}$$

where λ is the decay constant of ^{40}K and the asterisk identifies the radiogenic isotopes of K and Ca. The decay constant (λ) of ^{40}K is the sum of the decay constants that govern each of the two branches of the decay:

λ_e: electron-capture decay of ^{40}K to form ^{40}Ar*

λ_β: beta decay of ^{40}K to form ^{40}Ca*and the total decay constant of ^{40}K is:

$$\lambda = \lambda_e + \lambda_\beta \tag{3.2}$$

The decay of ^{40}K to ^{40}Ar is expressed by the equation:

$$^{40}\mathrm{Ar}^{*} = \frac{\lambda_e}{\lambda}\,{}^{40}\mathrm{K}\left(e^{\lambda t} - 1\right) \tag{3.3}$$

where λ_e/λ is the fraction of the ^{40}K atoms that decay to ^{40}Ar*. This equation can be used to date a K-bearing mineral, such as biotite or muscovite, by measuring the number of ^{40}Ar atoms that have accumulated in a unit weight of the mineral in the time that has elapsed since the mineral cooled sufficiently to allow the atoms of radiogenic ^{40}Ar to accumulate in its crystal lattice. In addition, the number of ^{40}K atoms that remain in the same unit weight of the mineral can be calculated from its measured potassium concentration.

The K-Ar method of dating arises from Eq. 3.3 which can be used to calculate the length of time in the past during which ^{40}Ar* has accumulated:

$$e^{\lambda t} = \left(\frac{^{40}Ar^{*}}{^{40}K}\right)\left(\frac{\lambda}{\lambda_e}\right) + 1$$

$$t = \frac{1}{\lambda}\ln\left[\left(\frac{^{40}Ar^{*}}{^{40}K}\right)\left(\frac{\lambda}{\lambda_e}\right) + 1\right] \tag{3.4}$$

Equation 3.4 can now be used to illustrate the calculation of the K-Ar date of a biotite extracted from a hand specimen of paragneiss collected at Gneiss Point along the coast of southern Victoria Land at 77°24'S, 163°44'E,. Analyses reported by Goldich et al. (1958) of this biotite sample yield:

$$^{40}\mathrm{Ar}^{*}/{}^{40}\mathrm{K} = 0.0333$$

The ratio of the decay constants has the numerical value:

$$\frac{\lambda}{\lambda_e} = \frac{5.543 \times 10^{-10}}{0.581 \times 10^{-10}} = 9.9540$$

Substituting into Eq. 3.4 yields:

$$t = \frac{1}{5.543 \times 10^{-10}}\ln\left[0.0333 \times 9.540 + 1\right]$$

$$t = \frac{\ln 1.31768}{5.543 \times 10^{-10}} = \frac{0.2758}{5.543 \times 10^{-10}} = 500 \times 10^{6}\ \text{years}$$

This date is the amount of time that has elapsed since the rock sample cooled sufficiently to allow radiogenic ^{40}Ar to accumulate in the biotite. This date is less than the time since crystallization of the mineral. Therefore, the rock is older than 500 × 10^6 years by an unknown amount of time depending on the cooling rate.

The date calculated above differs from the value of 520 million years reported by Goldich et al. (1958) because the values of the decay constant of ^{40}K used by these authors have been replaced by more accurate values in use at the present time. Nevertheless, this was the first age determination of a rock in Antarctica based on radioactivity. The date reported by Goldich et al. (1958) more than 50 years ago indicated that high-grade metamorphism of the basement rocks of the Transantarctic Mountains occurred during Middle Cambrian time (IUGS 2002).

3.6.3 Rb-Sr Method

Rubidium is an alkali metal that has two naturally occurring isotopes (^{85}Rb and ^{87}Rb), one of which is radioactive and decays to a stable isotope of strontium (Faure and Mensing 2005):

$$^{87}\mathrm{Rb} \rightarrow {}^{87}\mathrm{Sr}^{*} + \beta^{-} + \overline{\nu} + \mathrm{Q} \tag{3.5}$$

where β^- is a beta particle, $\overline{\nu}$ is an antineutrino, and Q is the energy liberated by the decay of one atom of ^{87}Rb. The number of ^{87}Sr* atoms that form by decay of ^{87}Rb in a closed system is expressed by means of the Law of Radioactivity:

$$^{87}\mathrm{Sr}^{*} = {}^{87}\mathrm{Rb}\left(e^{\lambda t} - 1\right) \tag{3.6}$$

where the decay constant $\lambda = 1.42 \times 10^{-11}$ year^{-1}. The total number of ^{87}Sr atoms in a unit weight of Rb-bearing mineral (e.g., biotite or muscovite) is:

$$^{87}\mathrm{Sr} = {}^{87}\mathrm{Sr_i} + {}^{87}\mathrm{Sr}^* \tag{3.7}$$

where $^{87}Sr_i$ is the number of atoms of this isotope that were incorporated into the Rb-bearing mineral at the time of its formation. Therefore,

$$^{87}\mathrm{Sr} = {}^{87}\mathrm{Sr_i} + {}^{87}\mathrm{Rb}(e^{\lambda t} - 1) \tag{3.8}$$

Each term of Eq. 3.8 is divided by the number of stable and non-radiogenic ^{86}Sr atoms of "ordinary" strontium:

$$\frac{^{87}Sr}{^{86}Sr} = \left(\frac{^{87}Sr}{^{86}Sr}\right)_i + \left(\frac{^{87}Rb}{^{86}Sr}\right)(e^{\lambda t} - 1) \tag{3.9}$$

This equation can be used to date Rb-bearing minerals by measuring their $^{87}Sr/^{86}Sr$ and $^{87}Rb/^{86}Sr$ ratios and by solving Eq. 3.9 for t based on the known value of λ and an assumed value of $(^{87}Sr/^{86}Sr)_i$:

$$t = \frac{1}{\lambda}\ln\left[\frac{^{87}Sr/^{86}Sr - (^{87}Sr/^{86}Sr)_i}{(^{87}Rb/^{86}Sr)} + 1\right] \tag{3.10}$$

The resulting dates may be systematically in error in cases where the measured $^{87}Sr/^{86}Sr$ ratio of the mineral has about the same magnitude as the initial $^{87}Sr/^{86}Sr$ ratio. In addition, radiogenic ^{87}Sr may escape from Rb-bearing minerals as a result of slow cooling or by subsequent contact metamorphism or by isotope exchange with Sr in brines that may permeate the rocks. The loss of radiogenic ^{87}Sr by these or other processes lowers Rb-Sr mineral dates and causes them to underestimate the crystallization age of the host rock.

These problems are avoided by the whole-rock Rb-Sr isochron method of dating because the radiogenic ^{87}Sr that may diffuse out of Rb-rich minerals is quantitatively retained in most cases within the grain boundaries and by other minerals in a sample of the whole rock. When Eq. 3.9 is applied to a suite of rock samples all of which have the same age t, had the same initial $^{87}Sr/^{86}Sr$ ratio at the time of formation, and neither gained nor lost radiogenic ^{87}Sr, their measured $^{87}Sr/^{86}Sr$ and $^{87}Rb/^{86}Sr$ ratios form points on a straight line. This line is an isochron because all the rock or mineral samples that plot on this line have the same age.

Another way to recognize this phenomenon is to re-examine Eq. 3.9. If t is a constant, then $e^{\lambda t}$-1 is also a constant and the equation defines a straight line of the form:

$$y = b + mx \tag{3.11}$$

where $y = {}^{87}Sr/^{86}Sr$, $x = {}^{87}Rb/^{86}Sr$, $b = (^{87}Sr/^{86}Sr)_i$, and $m = e^{\lambda t}-1$ is the slope of the line.

The Rb-Sr isochron method was used by Jones and Faure (1967) in Section 3.4.2 to date whole-rock samples and separated alkali feldspars of two Vanda porphyry dikes in Wright Valley. A least-squares regression of the data points in Fig. 3.14 yields a slope (m):

$$m = e^{\lambda t} - 1 = 0.006553$$

$$t = \frac{1}{\lambda}\ln(0.006553 + 1)$$

$$t = \frac{0.006531}{1.42 \times 10^{-11}} = 460 \times 10^6\ \mathrm{y}$$

Any sample of rock or mineral that does not satisfy the preconditions stated above does not plot on the isochron defined by a suite of cogenetic rocks that had the same initial $^{87}Sr/^{86}Sr$ ratio when they formed. Therefore, the goodness of fit of data points that define a Rb-Sr isochron is indicative of how well the assumptions of dating by this method are satisfied.

3.6.4 $^{40}Ar/^{39}Ar$ Partial-Release Dates

In order to date a potassium-bearing mineral by the $^{40}Ar/^{39}Ar$ method the sample is first irradiated by energetic neutrons in the core of a nuclear reactor (Faure and Mensing 2005). The neutrons interact with the nuclei of ^{39}K atoms and transform them into nuclei of ^{39}Ar by a nuclear reaction of the form:

$$^{39}_{19}\mathrm{K} + \mathrm{neutron} \rightarrow {}^{39}_{18}\mathrm{Ar} + \mathrm{proton} \tag{3.12}$$

The resulting concentration of ^{39}Ar in the irradiated sample can be used to calculate the concentration of ^{39}K it contains. After the irradiation, the sample is heated stepwise in a vacuum and the isotopic composition of

the Ar that is released at each step is measured with a gas-source mass spectrometer. The measured ratio of the argon isotopes is related to the age of the sample by the equation:

$$\frac{^{40}Ar*}{^{39}Ar} = \frac{e^{\lambda t} - 1}{J} \tag{3.13}$$

where λ is the total decay constant of potassium (Appendix 3.6.2) and J is a constant that depends on the flux and energy distribution of the neutrons used in the irradiation. The "J-factor" is determined by irradiating a flux monitor which is a mineral whose age was determined by another radiogenic-isotope geochronometer. Therefore, the measured $^{40}Ar^*/^{39}Ar$ ratio of the mineral to be dated can be used to solve Eq. 3.13 for t which yields a date in the past.

When the sample to be dated is heated stepwise at increasing temperatures, the $^{40}Ar/^{39}Ar$ ratios of the argon that is released can be used to calculate a series of dates which form a spectrum when they are plotted versus the temperature of each heating step. Experience has shown that the $^{40}Ar/^{39}Ar$ ratios in many cases increase with increasing temperature because the gas that is released at low temperature has lost some of its radiogenic ^{40}Ar while the mineral cooled after it crystallized. The argon that is released at higher temperatures originates from the interiors of mineral grains and therefore has not lost radiogenic ^{40}Ar. Therefore, the $^{40}Ar/^{39}Ar$ dates form a flat-topped plateau that records the time when the mineral cooled through its blocking temperature.

The $^{40}Ar/^{39}Ar$ method of dating was used by Felder and Faure (1990) to determine the age of hornblende crystals from a sample of the Carlyon Granodiorite in the Brown Hills of southern Victoria Land. The spectrum of dates in Fig. 3.16 has a well-developed plateau that yields an average date of 534 ± 6 Ma.

3.6.5 U-Pb Methods

The long-lived and naturally occurring isotopes of uranium (^{238}U and ^{235}U) and thorium (^{232}Th) each decay to a different stable radiogenic isotope of lead through lengthy chains of intermediate radioactive daughters:

$$^{238}\mathrm{U} \rightarrow {}^{206}\mathrm{Pb}, \lambda_1 = 1.55125 \times 10^{-10}\,\mathrm{y}^{-1}$$

$$^{235}\mathrm{U} \rightarrow {}^{207}\mathrm{Pb}, \lambda_2 = 9.8485 \times 10^{-10}\,\mathrm{y}^{-1}$$

$$^{232}\mathrm{Th} \rightarrow {}^{208}\mathrm{Pb}, \lambda_3 = 4.9475 \times 10^{-11}\,\mathrm{y}^{-1}$$

The growth of radiogenic isotopes of lead in minerals that contain uranium and thorium is expressed by equations derivable from the Law of Radioactivity (Faure and Mensing 2005):

$$\frac{^{206}Pb}{^{204}Pb} = \left(\frac{^{206}Pb}{^{204}Pb}\right)_i + \frac{^{238}U}{^{204}Pb}(e^{\lambda_1 t} - 1) \tag{3.14}$$

$$\frac{^{207}Pb}{^{204}Pb} = \left(\frac{^{207}Pb}{^{204}Pb}\right)_i + \frac{^{235}U}{^{204}Pb}(e^{\lambda_2 t} - 1) \tag{3.15}$$

$$\frac{^{208}Pb}{^{204}Pb} = \left(\frac{^{208}Pb}{^{204}Pb}\right)_i + \frac{^{232}Th}{^{204}Pb}(e^{\lambda_3 t} - 1) \tag{3.16}$$

where ^{204}Pb is the only non-radiogenic stable isotope of lead. In addition, the ratio of radiogenic ^{207}Pb to ^{206}Pb is expressed by combining Eqs. 3.14 and 3.15 where the asterisk identifies the radiogenic origin:

$$\left(\frac{^{207}Pb}{^{206}Pb}\right)^* = \frac{\frac{^{207}Pb}{^{204}Pb} - \left(\frac{^{207}Pb}{^{204}Pb}\right)_i}{\frac{^{206}Pb}{^{204}Pb} - \left(\frac{^{206}Pb}{^{204}Pb}\right)_i} = \frac{^{235}U}{^{238}U}\left(\frac{e^{\lambda_2 t} - 1}{e^{\lambda_1 t} - 1}\right) \tag{3.17}$$

The dates calculated from these equations based on analytical data of U-bearing minerals (e.g., zircon) are *discordant* in most cases either because of continuous or episodic loss of atoms of radiogenic lead or gain of uranium after crystallization. The oldest and most reliable dates are obtained from the ratio of radiogenic $^{207}Pb/^{206}Pb$ (Eq. 3.17) because the loss of radiogenic lead does not alter this ratio as much as the $^{206}Pb/^{204}Pb$ and $^{207}Pb/^{204}Pb$ ratios. Minerals containing thorium can be dated by the Th-Pb method (Eq. 3.16) although analytical difficulties discourage its use.

The loss of radiogenic lead atoms formed by decay of uranium is circumvented by an ingenious mathematical procedure that was devised by Wetherill (1963):

Equations 3.14 and 3.15 are each written in the form:

$$\frac{^{206}Pb*}{^{238}U} = e^{\lambda_1 t} - 1 \tag{3.18}$$

$$\frac{^{207}Pb*}{^{235}U} = e^{\lambda_2 t} - 1 \qquad (3.19)$$

These equations are used to calculate compatible sets of $^{206}Pb^*/^{238}U$ and $^{207}Pb^*/^{235}U$ ratios for selected values of t. The resulting values of these ratios are the coordinates of points that define the *concordia* curve which is the locus of all points whose coordinates yield concordant U-Pb dates. Any point that represents a mineral whose measured $^{206}Pb^*/^{238}U$ and $^{207}Pb^*/^{235}U$ ratios do not plot on concordia yield discordant U-Pb dates which are not valid age determinations.

Experience has shown that the $^{206}Pb^*/^{238}U$ and $^{207}Pb^*/^{235}U$ ratios of zircons extracted from the same body of rock define a straight-line *discordia* chord that intersects the concordia curve at two points. The coordinates of these points yield concordant dates because they lie on concordia. Several alternative explanations have been proposed to explain why zircons that yield discordant U-Pb dates nevertheless define a straight-line chord on the concordia diagram (Faure and Mensing 2005). The simplest but not necessarily the only explanation is that the discordance of U-bearing minerals is caused either by loss of radiogenic lead or by gain or loss of uranium. In any case, the dates calculated from the coordinates of the upper intercept are considered to be either the time of original crystallization of the U-bearing mineral or the time when the mineral was so severely altered that all radiogenic lead was lost. The lower intercept, in some cases, dates an episode of partial loss of radiogenic lead which should be confirmed by K-Ar and Rb-Sr dates of coexisting mica minerals (Appendices 3.6.2 and 3.6.3). If the chord intersects concordia at the origin, then the loss of radiogenic lead is occurring as a result of chemical weathering at the present time. The concordia diagram in Fig. 3.17 illustrates the case presented by Vocke and Hanson (1981) for zircons they extracted from the Olympus Granite-Gneiss in DVDP core 6 drilled at Lake Vida in Victoria Valley of southern Victoria Land.

3.6.6 Sm-Nd Method

Samarium (Sm) and neodymium (Nd) are rare earth elements (REE) that are widely distributed in rocks composed of silicate minerals (Faure and Mensing 2005). One of the naturally occurring isotopes of Sm is radioactive and decays to a stable isotope of Nd by emitting alpha particles (nuclei of $^4_2$He):

$$^{147}_{62}\mathrm{Sm} \rightarrow ^{143}_{60}\mathrm{Nd} + ^4_2\mathrm{He} + \mathrm{energy} \qquad (3.20)$$

The halflife of ^{147}Sm is 1.06×10^{11} years which corresponds to a decay constant of $\lambda = 6.54 \times 10^{-12}$ year^{-1}.

The growth of radiogenic ^{143}Nd is expressed by an equation derived from the Law of Radioactivity:

$$\frac{^{143}Nd}{^{144}Nd} = \left(\frac{^{143}Nd}{^{144}Nd}\right)_i + \left(\frac{^{147}Sm}{^{144}Nd}\right)(e^{\lambda t} - 1) \qquad (3.21)$$

This equation is used for dating suites of Sm-bearing rocks by the isochron method used also for dating comagmatic igneous rocks by the Rb-Sr method.

The Sm-Nd method can be used to date mafic igneous rocks (basalt and gabbro) which are not suitable for dating by the Rb-Sr method. Magma of basaltic chemical composition originates by decompression melting in the mantle of the Earth which contains radiogenic ^{143}Nd that has formed by decay of ^{147}Sm. The isotopic evolution of Nd in the mantle of the Earth is represented by a model in Fig. 3.19 that is based on the isotope composition of neodymium in chondrite meteorites and which is therefore known as the "Chondritic Uniform Reservoir" (CHUR). The present value of the $^{143}Nd/^{144}Nd$ ratio in CHUR is:

$$\left(\frac{^{143}Nd}{^{144}Nd}\right)^0_{CHUR} = 0.512638$$

where the superscript "0" indicates that it applies to the present time (i.e., t = 0). The $^{147}Smd/^{144}Nd$ ratio of CHUR is:

$$\left(\frac{^{147}Sm}{^{144}Nd}\right)^0_{CHUR} = 0.1967$$

and the initial $^{143}Nd/^{144}Nd$ ratio of CHUR at $t = 4.5 \times 10^9$ years ago is:

$$\left(\frac{^{143}Nd}{^{144}Nd}\right)^t_{CHUR} = 0.506764$$

The increase of the $^{143}Nd/^{144}Nd$ ratio of CHUR as a function of time is indicated in Fig. 3.19.

The model for the isotopic evolution of Nd in the mantle of the Earth (i.e., CHUR) can be used to calculate the time when the Nd in a crustal rock was separated from the "chondritic reservoir." This calculation is made by adapting Eq. 3.21:

$$0.512638 = \left(\frac{^{143}Nd}{^{144}Nd}\right)_i + 0.1967(e^{\lambda t} - 1) \quad (3.22)$$

which can be solved for t based on the initial $^{143}Nd/^{144}Nd$ ratio obtained from a Sm-Nd isochron of a suite of comagmatic igneous rocks:

$$t = \frac{1}{6.54 \times 10^{-12}} \ln\left[\frac{0.512638 - (^{143}Nd\,/^{144}\,Nd)_i}{0.1967} + 1\right] \quad (3.23)$$

The analytical data of Rowell et al. (1993) for a whole-rock sample and magnetic fractions of a pillow basalt in the Cocks Formation in the Skelton Glacier area define a Sm-Nd isochron in Fig. 3.18 which yields an initial $^{143}Nd/^{144}Nd$ ratio of 0.511594. Substituting this value into Eq. 3.23 yields:

$$t = \frac{1}{6.54 \times 10^{-12}} \ln\left[\frac{0.512638 - 0.511594}{0.1967} + 1\right]$$

$$t = \frac{\ln 1.0053075}{6.54 \times 10^{-12}} = 809 \times 10^6\,\text{y}$$

The procedure by which this date was obtained is more transparent than the method used by Rowell et al. (1993) who obtained dates between 700 and 800 Ma.

References

Adams CJ, Whitla PF (1991) Precambrian ancestry of the Asgard Formation (Skelton Group): Rb-Sr age of basement metamorphic rocks in the Dry Valley region, Antarctica. In: Thomson MRA, Crame JA, Thomson JW (eds) Geological evolution of Antarctica. Cambridge University Press, Cambridge, pp 129–135

Allen AD, Gibson GW (1962) Geological investigations in southern Victoria Land, Antarctica. Part 6: Outline of the geology of the Victoria Valley region. New Zealand J Geol Geophys 5:234–242

Allibone AH, Cox SC, Graham IJ, Smillie RW, Johnstone RD, Ellery SG, Palmer K (1993a) Granitoids of the Dry Valleys area, southern Victoria Land, Antarctica: Plutons, field relationships, and isotopic dating. New Zealand J Geol Geophys 36:281–297

Allibone AH, Cox SC, Smillie RW (1993b) Granitoids of the Dry Valleys area, southern Victoria Land: Geochemistry and evolution along the early Paleozoic Antarctic craton margin. New Zealand J Geol Geophys 36:299–316

Angino EE, Turner MD (1964) Antarctic orogenic history from absolute age dates. In: Adie RJ (ed) Antarctic geology. North-Holland, Amsterdam, The Netherlands, pp 552–556

Angino EE, Turner MD, Zeller EJ (1960) Reconnaissance geology of the Mt. Nussbaum area, Taylor Dry Valley, Victoria Land, Antarctica. Geol Soc Amer Bull 71(12):1816

Angino EE, Turner MD, Zeller EJ (1962) Reconnaissance geology of lower Taylor Valley, Victoria Land, Antarctica. Geol Soc Amer Bull 73:1553–1562

Bell RT, Jefferson CW (1987) An hypothesis for an Australian-Canadian connection in the Late Proterozoic and the birth of the Pacific Ocean. Proceedings of the Pacific-Rim Congress, 1987, Parkville, Victoria, 39–50, Australian Inst. Mining and Metallurgy

Berger GW, York D (1981) Geothermometry from $^{40}Ar/^{39}Ar$ dating experiments. Geochim Cosmochim Acta 45:795–812

Blank HR, Cooper RA, Wheeler RH, Willis IAG (1963) Geology of the Koettlitz-Blue Glacier region, southern Victoria Land, Antarctica. Trans Roy Soc New Zealand Geol 2(5):79–100

Bodley FA (ed) (1968) Fifth special Antarctic issue. New Zealand J Geol Geophys 11(4):791–1076

Borg SG, DePaolo DJ (1991) A tectonic model of the Antarctic Gondwana margin with implications for southeast Australia: Isotopic and geochemical evidence. Tectonophys 196: 339–358

Borg SG, DePaolo DJ (1994) Laurentia, Australia, and Antarctica as a Late Proterozoic supercontinent: Constraints from isotopic mapping. Geol 22:307–310

Bradshaw JD, Weaver SD, Laird MD (1985) Suspect terranes and Cambrian tectonics in northern Victoria Land, Antarctica. In: Howell DG (ed) Tectonostratigraphic Terranes of the Circum Pacific Region. Circum-Pacific Council for Energy Mineral Resources, Houston, TX, pp 467–479

Bull C (1962) Gravity observations in the Koettlitz Glacier area, southern Victoria Land, Antarctica. New Zealand Geol Geophys 5:810–819

Bull C (1966) Climatological observations in the ice-free areas of southern Victoria Land, Antarctica. In: Rubin MJ (ed) Studies in Antarctic Meteorology. Antarctic Research Series, vol. 9. American Geophysical Union, Washington, DC, pp 177–194

Calkin PE (1974) Subglacial geomorphology surrounding the ice-free valleys of southern Victoria Land, Antarctica. J Glaciol 13(69):415–429

Collins BW (ed) (1962) Special Antarctic issue. New Zealand J Geol Geophys 5(5):671–672

Collins BW (ed) (1963) Special Antarctic issue. New Zealand J Geol Geophys 6(3):305–306

Collins BW (ed) (1965) Third special Antarctic issue. New Zealand J Geol Geophys 8(2):163–390

Collins BW (ed) (1967) Fourth special Antarctic issue. New Zealand J Geol Geophys 10(2):307–623

Cox SC (1993) Inter-related plutonism and deformation in southern Victoria Land, Antarctica. Geol Mag 130:1–14

Craddock C (ed) (1969a) Geologic maps of Antarctica. Antarctic Folio Series, Folio 12. American Geographic Society, New York

Craddock C (1969b) Radiometric age map of Antarctica. Antarctic Map Folio Series, Folio 12, Plate 19, American Geographical Society, New York

Craddock C (ed) (1982) Antarctic geoscience. University of Wisconsin Press, Madison, WI

Dahl PS, Palmer DF (1981) Field study of orbicular granitic rocks in Taylor Valley, southern Victoria Land. Ant J US 16(6):47–49

Dahl PS, Palmer DF (1983) The petrology and origin of orbicular tonalite from western Taylor Valley, southern Victoria Land, Antarctica. In: Oliver RJ, James PR, Jago JB (eds) Antarctic Earth Science. Australian Academy of Science, Canberra, ACT, pp 156–159

Dallmeyer RD, Hess JR, Whitney JA (1981) Post-magmatic cooling of the Elberton Granite; Bearing on the Paleozoic tectonothermal history of the Georgia inner piedmont. J Geol 89:585–600

Dalziel IWD (1991) Pacific margin of Laurentia and East Antarctica-Australia as a conjugate rift pair: Evidence and implications for an Eocambrian supercontinent. Geology 19:598–601

Denton GH, Armstrong RL, Stuiver M (1970) Late Cenozoic glaciation in Antarctica; The record in the McMurdo Sound region. Antarctic J US 5:15–21

Deutsch S, Webb PN (1964) Sr/Rb dating on basement rocks from Victoria Land; Evidence for a 1000 million year old event. In: Adie RJ (ed) Antarctic geology. Wiley, New York, pp 557–562

Deutsch S, Grőgler N (1966) Isotopic age of Olympus Granite–Gneiss (Victoria Land, Antarctica). Earth Planet. Sci. Letters, 1:82–84

Elliot DH (1975) Tectonics of Antarctica: A review. Amer J Sci 275-A:45–106

Encarnación J, Grunow A (1996) Changing magmatic and tectonic styles along the paleo-Pacific margin of Gondwana and the onset of early Paleozoic magmatism in Antarctica. Tectonics 15(6):1325–1341

Fairbridge RW (1975) Antarctica. In: Fairbridge RW (ed) The Encyclopedia of World Regional Geology, Part 1; Western Hemisphere (Including Antarctica and Australia). Dowden, Hutchinson & Ross, Stroudsburg, PA, pp 2–13

Faure G (2001) Origin of igneous rocks; The isotopic evidence. Springer, Heidelberg, Germany

Faure G, Mensing TM (2005) Isotopes; Principles and applications. Wiley, Hoboken, NJ

Faure G, Jones LM, Owen LB (1974) Isotopic composition of strontium and geologic history of the basement rocks of Wright Valley, southern Victoria Land, Antarctica. New Zealand J Geol Geophys 17(3):611–627

Felder RP (1980) Geochronology of the Brown Hills, Transantarctic Mountains. M.Sc. thesis, Department of Geology and Mineral Industries, The Ohio State University, Columbus, Ohio

Felder RP, Faure G (1980) Rubidium-strontium age determinations of part of the basement complex of the Brown Hills, central Transantarctic Mountains. Antarctic J US 15(5):16–17

Felder RP, Faure G (1990) Age and petrogenesis of the granitic basement rocks, Brown Hills, Transantarctic Mountains. In: Miller H (ed) Workshop on Antarctic Geochronology. Zentralblatt fűr Geologie und Paläontology, Teil I, vol. 1990 (1/2), pp 45–62

Ferracioli F, Bozzo E, Capponi G (2002) Aeromagnetic and gravity constraints for an early Paleozoic subduction system of Victoria Land, Antarctica. Geophys Res Lett 29(10):1406

Findlay RH, Skinner DNB, Craw D (1984) Lithostratigraphy and structure of the Koettlitz Group, McMurdo Sound, Antarctica. New Zealand J Geol Geophys 27:513–536

Findlay RH, Unrug R, Banks MR, Veevers JJ (eds) (1993) Gondwana Eight; Assembly, evolution, and dispersal. Balkema, Rotterdam, The Netherlands

Flory RF, Murphy DJ, Smithson SB, Houston RS (1971) Geologic studies of basement rocks in southern Victoria Land. Antarctic J US 6(4):119–120

Ford AB (1964) Review of Antarctic geology. Trans Amer Geophys Union 45:363–381

Friedmann EI, Hua M, Ocampo-Friedmann R (1988) Cryptoendolithic and cyanobacterial communities of the Ross Desert, Antarctica. Polarforschung 58:251

Fűtterer DK, Damaske D, Kleinschmidt G, Miller H, Tessensohn F (1996) Antarctica; Contributions to global Earth sciences. Springer, Berlin/Heidelberg, Germany

Gamble JA, Skinner DNB, Henrys S (eds) (2002) Antarctica at the close of the millennium. Roy Soc New Zealand Bull 35:251–259

Ghent ED, Henderson RA (1968) Geology of the Mt. Falconer pluton, lower Taylor Valley, south Victoria Land, Antarctica. New Zealand J Geol Geophys 11(4):851–880

Goldich SS, Nier AO, Washburn AL (1958) $^{40}Ar/^{40}K$ age of gneiss from McMurdo Sound, Antarctica. Trans Amer Geophys Union 39(8):956–958

Graham IJ, Palmer K (1987) New precise Rb-Sr mineral and whole-rock dates for I-type granitoids from Granite Harbor, south Victoria Land, Antarctica. New Zealand Antarctic Record 8(1):72–80

Grikurov GE (1982) Structure of Antarctica and outline of its evolution. In: Craddock C (ed) Antarctic geoscience. University of Wisconsin Press, Madison, WI, pp 791–804

Grindley GW (1971) Polyphase deformation of the Precambrian Nimrod Group, central Transantarctic Mountains. In: Adie RJ (ed) Antarctic geology and geophysics, Universitetsforlaget, Oslo, Norway

Grindley GW (1981) Precambrian rocks of the Ross Sea region. J Roy Soc New Zealand 11(4):411–423

Grindley GW, Laird MG (1969) Geology of the Shackleton Coast. In: Craddock C (ed) Geologic maps of Antarctica, Folio 12, Sheet 15. American Geographical Society, New York

Grindley GW, Warren G (1964) Stratigraphic nomenclature and correlation in the western Ross Sea region. In: Adie RJ (ed) Antarctic geology. North- Holland, Amsterdam, The Netherlands, pp 314–333

Grunow A, Hanson R, Wilson TJ (1996) Were aspects of Pan-African deformation linked to Iapetus opening? Geol 24(12):1063–1066

Gunn BM (1963) Geological structure and stratigraphic correlation in Antarctica. New Zealand J Geol Geophys 6(3):423–443

Gunn BM, Walcott RI (1962) The geology of the Mount Markham region, Ross Dependency, Antarctica. New Zealand J Geol Geophys 5(3):407–426

Gunn BM, Warren G (1962) Geology of Victoria Land between the Mawson and the Mullock Glaciers, Antarctica. New Zealand Geol Surv Bull 71:1–157

Hamilton PJ, Evensen NM, O'Nions RK, Smith HS, Erlank AJ (1979) Sm-Nd dating of Onverwacht Group volcanics, Southern Africa. Nature 279:25–28

Hamilton W (1967) Tectonics of Antarctica. Tectonophysics 4(4/6):555–568

Hamilton W, Hayes PT (1960) Geology of the Taylor Glacier-Taylor dry valley region, south Victoria Land, Antarctica. US Geol Surv Prof. Paper 400-B:376–377

Harrington HJ (1958) Nomenclature of rock units in the Ross Sea region, Antarctica. Nature 182:290

Haskell TR, Kennett JP, Prebble WM (1964) Basement and sedimentary geology of the Darwin Glacier area, Antarctica. In: Adie RJ (ed) Antarctic geology. North-Holland, Amsterdam, The Netherlands, pp 348–351

Haskell TR, Kennett JP, Prebble WM, Smith G, Willis IAG (1965a) The geology of the middle and lower Taylor Valley of south Victoria Land, Antarctica. Trans Roy Soc New Zealand 2(12):169–186

Haskell TR, Kennett JP, Prebble WM (1965b) Geology of the Brown Hills and Darwin Mountains, southern Victoria Land. Trans Roy Soc New Zealand 2(15):231–248

Heimann A, Fleming TH, Elliot DH, Foland KA (1994) A short interval of Jurassic continental flood basalt volcanism in Antarctica as demonstrated by $^{40}Ar/^{39}Ar$ geochronology. Earth Planet Sci Lett 121:19–41

Herbert WW (1962) The Axel-Heiberg Glacier. New Zealand J Geol Geophys 5(5):681–706

Houtzager G (2003) The complete encyclopedia of Greek mythology. Chartwell Books, Edison, NJ

IUGS (2002) International stratigraphic chart. Commission on the Geologic Map of the World, UNESCO, United Nations, New York

Jackson JA (ed) (1997) Glossary of geology, 4th edn. American Geological Institute, Alexandria, VA

Jones LM, Faure G (1967) Age of the Vanda Porphyry dikes in Wright Valley, southern Victoria Land, Antarctica. Earth Planet. Sci. Letters, 3:321–324

Kurasawa H, Yoshida Y, Mudrey MG Jr (1974) Geological log of the Lake Vida core-DVDP 6. In: Dry Valley Drilling Project, Bulletin 3. DeKalb, Northern Illinois University, DeKalb, IL, pp 92–108

Kyle PR (ed) (1995) Volcanological and environmental studies of Mt. Erebus, Antarctica. Antarctic Research Series, vol. 66. American Geophysical Union, Washington, DC

Laird MB (1981) Lower Paleozoic rocks of Antarctica. In: Holland CH (ed) Lower Paleozoic of the Middle East, Eastern and Southern Africa, and Antarctica. Wiley, London, pp 257–314

Laird MG, Bradshaw JD (1982) Uppermost Proterozoic and lower Paleozoic geology of the Transantarctic Mountains. In: Craddock C (ed) Antarctic Geoscience. University of Wisconsin Press, Madison, WI, pp 525–533

LeMasurier WE, Thomson JW (eds) (1990) Volcanoes of the Antarctic plate and southern Oceans. Antarctic Research Series, vol. 48. American Geophysical Union, Washington, DC

Mayewski PA, Goldthwait RP (1985) Glacial events in the Transantarctic Mountains: A record of the East Antarctic ice sheet. In: Turner MD, Splettstoesser JF (eds) Geology of the Transantarctic Mountains. Antarctic Research Series, vol. 36, Paper 12. American Geophysical Union, Washington, DC, pp 275–324

McDougall I, Ghent ED (1970) Potassium-argon dates on minerals from the Mt. Falconer area, lower Taylor Valley, south Victoria Land, Antarctica. New Zealand J Geol Geophys 13(4):1026–1029

McKelvey BC, Webb PN (1959) Geological investigations in south Victoria Land, Antarctica. Part 2: Geology of the upper Taylor Glacier region. New Zealand J Geol Geophys 2(4):718–728

McKelvey BC, Webb PN (1962) Geological investigations in southern Victoria Land, Antarctica. New Zealand J Geol Geophys 5:143–162

Moores EM (1991) Southwest U.S.-East Antarctic (SWEAT) connection: A hypothesis. Geol 19:425–428

Mortimer G (1981) Provisional report on the geology of the basement complex between Miers and Salmon Valley, McMurdo Sound, Antarctica. New Zealand Antarctic Record 3(2):1–8

Murphy DJ, Flory RF, Houston RS, Smithson SB (1970) Geological studies of basement rocks in south Victoria Land. Antarctic J US 5(4):102

Nichols RL (1963) Geologic features demonstrating aridity of the McMurdo Sound area, Antarctica. Amer J Sci 261:20–31

Palmer DF, Bradley J, Prebble WM (1967) Orbicular granodiorite from Taylor Valley, south Victoria Land, Antarctica. Geol Soc Amer Bull 78:1423–1428

Pearn WC, Angino EE, Stewart D (1963) New isotopic age measurements from the McMurdo Sound area, Antarctica. Nature 199:685

Péwé TL (1960) Multiple glaciation in the McMurdo Sound region, Antarctica: A progress report. J Geol 68:498–514

Picciotto E, Coppez A (1962) Bibliographie des mesures d'ages absolus en Antarctique. Annales Soc Geol Belg 85(8):263–308

Picciotto E, Coppez A (1964a) Bibliographie des mesures d'ages absolus en Antarctique (addendum, aout 1963). Ann Soc Geol Belg 85(4):115–128

Picciotto E, Coppez A (1964b) Bibliography of absolute age determinations in Antarctica (addendum). In: Adie RJ (ed) Antarctic geology. North-Holland, Amsterdam, The Netherlands, pp 563–569

Quartermain LB (1963) Publications resulting from work done under the aegis of the New Zealand Antarctic Research Programmes 1956–1962. New Zealand J Geol Geophys 6(3):348–360

Quartermain LB (1965) Publications resulting from work done under the aegis of the New Zealand Antarctic Research Programmes 1963–1964. New Zealand J Geol Geophys 8(2):371–379

Ravich MG, Ya Krylov A (1964) Absolute ages of rocks from East Antarctica. In: Adie RJ (ed) Antarctic geology. North-Holland, Amsterdam, The Netherlands, pp 491–494

Rees MN, Duebendorfer EM, Rowell AJ (1989) The Skelton Group, southern Victoria Land. Antarctic J US 24(5):21–24

Rowell AJ, Rees MN, Duebendorfer EM, Wallin ET, VanSchmus WR, Smith EI (1993) An active Neoproterozoic margin: Evidence from the Skelton Glacier area, Transantarctic Mountains. J Geol Soc London 150:677–682

Rowley PD (1983) Developments in Antarctic geology during the past half century. In: Boardman SJ (ed) Revolution of the

earth sciences; advances in the past half-century. Kendall/Hunt, Dubuque, IA
Schmidt DL (1966) The Transantarctic Mountains. Geotimes (November):15–16
Skinner DNB (1982) Stratigraphy and structure of low-grade metasedimentary rocks of the Skelton Group, southern Victoria Land; Does the Teall graywacke really exist? In: Craddock C (ed) Antarctic geoscience. University of Wisconsin Press, Madison, WI, pp 555–563
Smithson SB, Murphy DJ, Houston RS (1971a) Development of an augen-gneiss terrain. Contrib Mineral Petrol 33: 184–190
Smithson SB, Fikkan PR, Murphy DR, Houston RS (1971b) Development of augen-gneiss in the ice-free valley area, south Victoria Land. In: Adie RJ (ed) Antarctic geology and geophysics. Universitetsforlaget, Oslo, Norway, pp 293–298
Smithson SB, Fikkan PR, Houston RS (1971c) Amphibolitization of calc-silicate metasedimentary rocks. Contrib Mineral Petrol 31:228–237
Steiger RH, Jäger E (1977) Subcommission on geochronology: Convention on the use of decay constants in geo- and cosmochronology. Earth Planet Sci Lett 36:359–362
Stonehouse B (ed) (2002) Encyclopedia of Antarctica and the Southern Oceans. Wiley, Chichester
Streckeisen AL (1967) Classification and nomenclature of igneous rocks. Neues Jahrbuch Miner. Abhandlungen 107(2/3):144–240
Streckeisen AL (1976) To each plutonic rock its proper name. Earth Sci Rev 12:1–33
Stuckless JS, Ericksen RL (1975) Rb-Sr ages of basement rocks recovered from borehole DVDP 6, southern Victoria Land, Antarctica. Antarctic J US 10(6):301–307
Studinger M, Bell RE, Buck R, Karner GD, Blankenship DD (2004) Sub-ice geology inland of the Transantarctic Mountains in light of new aerogeophysical data. Earth Planet Sci Lett 220:391–408
Stuiver M, Braziunas TF (1985) Compilation of isotopic dates from Antarctica. Radiocarbon 27(2A):117–304
Stump E (1995) The Ross Orogen of the Transantarctic Mountains. Cambridge University Press, New York
Swithinbank C (1988) Antarctica. U.S. Geol. Surv. Prof. Paper 1386-B. U.S. Government Printing Office, Washington, DC
Tingey RJ (ed) (1991) The geology of Antarctica. Clarendon, Oxford
Tingey RJ (1996) How the south was won: A review of the first 150 years of Antarctic geologic exploration. Terra Antartica 3:1–10
Vocke RD Jr, Hanson GN (1981) U-Pb zircon ages and petrogenetic implications for two basement units from Victoria Valley, Antarctica. In: McGinnis LD (ed) Dry Valley drilling project. Antarctic Research Series, vol. 33. American Geophysical Union, Washington, DC, pp 247–255
Vocke RD Jr, Hanson GN, Stuckless JS (1978) Ages of the Vida granite and the Olympus granite gneiss, Victoria Valley, southern Victoria Land. Antarctic J US 13:15–17
Wade FA, Yeats VL, Everett JR, Greenlee DW, LaPrade KE, Shenk JC (1965) The geology of the central Queen Maud Range, Transantarctic Mountains, Antarctica. Antarct. Rept. Ser., 65–1. Texas Tech. Coll., Lubbock, TX
Warren G (1969) Geology of the Terra Nova Bay-McMurdo Sound area, Victoria Land. In: Craddock C (ed) Geologic maps of Antarctica, Folio 12, Sheet 14, American Geographical Society, New York
Webb PN (1962) Isotope dating of Antarctic rocks. A summary, I. New Zealand J Geol Geophys 5(5):790–796
Webb PN, McKelvey BC (1959) Geological investigations in south Victoria Land, Antarctica. Part 1: Geology of Victoria Valley. New Zealand J Geol Geophys 2(1):120–136
Webb PN, Warren G (1965) Isotope dating of Antarctic rocks, II. New Zealand J Geol Geophys 8(2):221–230
Wetherill GW (1963) Discordant uranium-lead ages, part 2: Discordant ages resulting from diffusion of lead and uranium. J Geophys Res 68:2957–2965
Williams PF, Hobbs BE, Vernon RH, Anderson DE (1971) The structural and metamorphic geology of basement rocks in the McMurdo Sound area, Antarctica J Geol Soc Australia 18(2):127–142

Springer

http://www.springer.com/978-1-4020-8406-5

The Transantarctic Mountains
Rocks, Ice, Meteorites and Water
Faure, G.; Mensing, T.M.
2011, X, 600 p., Hardcover
ISBN: 978-1-4020-8406-5